Draft version February 1, 2008
Preprint typeset using LaTeX style emulateapj v. 04/03/99

arXiv:astro-ph/9909128v1 7 Sep 1999

SPECTROSCOPY AND TIME VARIABILITY OF ABSORPTION LINES IN THE DIRECTION OF THE VELA SUPERNOVA REMNANT[1]

Alexandra N. Cha[2] & Kenneth R. Sembach[2]

Draft version February 1, 2008

ABSTRACT

We present high resolution (R≈75,000), high signal-to-noise (S/N≈100) Ca II λ3933.663 and Na I $\lambda\lambda$5889.951, 5895.924 spectra of 68 stars in the direction of the Vela supernova remnant. The spectra comprise the most complete high resolution, high S/N, optical survey of early type stars in this region of the sky. A subset of the sight lines has been observed at multiple epochs, 1993/1994 and 1996. Of the thirteen stars observed twice, seven have spectra revealing changes in the equivalent width and/or velocity structure of lines, most of which arise from remnant gas. Such time variability has been reported previously for the sight lines towards HD 72089 and HD 72997 by Danks & Sembach (1995) and for HD 72127 by Hobbs *et al.* (1991). We have confirmed the ongoing time variability of these spectra and present new evidence of variability in the spectra of HD 73658, HD 74455, HD 75309 and HD 75821. We have tabulated Na I and Ca II absorption line information for the sight lines in our sample to serve as a benchmark for further investigations of the dynamics and evolution of the Vela SNR.

Subject headings: line: profiles – ISM: clouds – ISM: individual (Vela Supernova Remnant) – ISM: supernova remnants – ISM: kinematics and dynamics

1. INTRODUCTION

The Vela supernova remnant (SNR), located in the Southern Milky Way at $l \approx 264°$, $b \approx -3°$ at a distance of 250±30 pc (Cha, Sembach, & Danks 1999 – Paper I), is a bright extended X-ray source that is roughly spherical in shape with an angular diameter of 7.3° (Aschenbach 1993). In the infrared, the remnant appears patchy indicating a disparity in the concentration of dust throughout the region. Near the center of the Vela SNR is the Vela pulsar, a radio bright source thought to be the remains of the star that exploded to create the SNR approximately 11,000 years ago (Reichley *et al.* 1970). In projection, several other structures are in close proximity to the Vela SNR, including the Gum Nebula, the Vela Molecular Ridge, SNR RX J0852.0 – 4622, and the Vela IRAS Shell.

The combination of the large size of the Vela SNR with the presence of many early type stars in this region of the sky has allowed the remnant gas to be studied through optical absorption line spectroscopy (Wallerstein & Silk 1971; Wallerstein *et al.* 1980; Jenkins *et al.* 1984; Hobbs *et al.* 1991; Danks & Sembach 1995). New high resolution (R ≈ 75,000), high signal-to-noise (S/N ≥ 100) Ca II and Na I spectra of over 60 stars in the direction of the Vela SNR are presented herein. With this data set, we measured a distance of 250±30 pc to the Vela SNR by noting which spectra contain moderate to high velocity ($V_{LSR} \geq 25$ km s^{-1}) lines associated with shocked SNR gas (Paper I).

Multi-epoch observations of some stars towards the Vela SNR have also enabled a study of the temporal variability of the high velocity remnant gas. Unlike the spectra of most sight lines in the sky, the Ca II and Na I absorption spectra for several sight lines that penetrate the Vela SNR change on timescales of a few years. For instance, the spectra of these ions towards the binary star HD 72127 fluctuated throughout an eight year observing campaign pursued by Hobbs *et al* (1991). Danks & Sembach (1995) also reported time variability towards two stars in the direction of the remnant, HD 72089 and HD 72997.

The variable nature of the interstellar absorption lines in this region of the sky provides a unique opportunity to study the ongoing kinetic and chemical evolution of the SNR. In this paper, we identify several sight lines exhibiting variability and provide a set of high quality observations from which further absorption line studies of the remnant may be pursued. The data acquisition and reduction methods are outlined in §§2 and 3. A description of the region surrounding the Vela SNR is given in §4. In §5 the absorption line spectra for the stars in the sample are presented. Additionally, the measured line widths and velocities obtained from our spectra and from previously published studies of Ca II and Na I have been tabulated to provide a broader context in which to study the remnant. For sight lines that exhibit time variability, multiple spectra from different observing runs are compared. A discussion of the physical mechanisms at work in the gas responsible for the temporal changes in the absorption components is in §6. Concluding remarks are contained in §7.

2. OBSERVATIONS AND SAMPLE INFORMATION

High-resolution optical spectra of 68 OB stars were obtained using the Coudé Echelle Spectrograph (CES) on the 1.4 meter Coudé Auxiliary Telescope (CAT) at the European Southern Observatory in February of 1993, February of 1994, and January/February of 1996. The instrumental setup was similar for each observing run. The spectrograph was outfitted with the "short" camera and either an RCA CCD (ESO#9, 1993, 1994) or a Loral CCD (ESO#38, 1996). We employed two different configura-

[1]Based on observations obtained at the European Southern Observatory, La Silla, Chile

[2]Department of Physics & Astronomy, The Johns Hopkins University, Baltimore, MD 21218; e-mail: *zan@pha.jhu.edu, sembach@pha.jhu.edu*

tions of the CES to observe either the Ca II λ3933.663 (K) or Na I $\lambda\lambda$5889.951, 5895.924 (D_2, D_1) and He I λ5875.618 lines. The wavelength coverage of the single echelle order observed in each setup was approximately 31Å (Ca II) or 50Å (Na I). Additional details about the CAT/CES can be found in Dekker *et al.* (1986) and Kaper & Pasquini (1996).

Multiple observations of 15–40 minutes in duration were made for each star. In some cases, sight lines were observed at different epochs to search for time variability in the absorption lines associated with Vela SNR gas. The fully reduced data have high signal-to-noise ratios, typically S/N $\geq$ 100. The spectra have a 2-pixel resolution $\lambda/\Delta\lambda \approx 75{,}000$, or $\approx$4 km s^{-1}, as determined from the widths of the thorium-argon lamp calibration spectra taken each night (see §3).

Table 1 lists the 68 OB stars observed along with information about their Galactic positions (longitude and latitude), MK classifications, visual magnitudes, observed photometric colors, B–V color excesses, distances, heliocentric radial velocities (v_{rad}), and projected rotational velocities ($v\,sin\,i$). Spectral types from a variety of sources were adopted (see the endnotes for Table 1), with preference given to MK classifications by Garrison, Hiltner, & Schild (1977) and Hiltner, Garrison, & Schild (1969). Whenever possible, classifications based upon slit spectra were used, but in several cases it was necessary to rely upon objective prism spectral classifications (Houk 1978). A colon is attached to the MK types listed in Table 1 determined by the latter method. Comparison of the adopted classifications with others in the literature shows that they are generally reliable to a class in both spectral type and luminosity, with correlated variations (in the sense that hotter main sequence stars were sometimes classified as cooler, more luminous stars). The impact of these classification differences in spectral type and luminosity on our derived spectroscopic distance estimates for the stars is reduced by these correlations. The photometric colors in Table 1 also came from a number of sources, with preference given to values from Schild, Garrison, & Hiltner (1983), Deutschman, Davis, & Schild (1976), and Johnson *et al.* (1966). Variations in these colors from one author to the next were typically 0.02 magnitudes or less. In a few cases, no published photometric colors other than those in the HD catalog exist. A colon follows these values in Table 1 and they are listed to a single decimal place.

The radial velocities in Table 1 are from Evans (1979), Wilson (1953), and Denoyelle (1987) and the projected rotational velocities are from Uesugi & Fukuda (1982). Values of v_{rad} and $v\,sin\,i$ in parentheses are estimates based on the centroids and full widths at half maximum intensity of the stellar He I λ5875.618 lines in our spectra when no previously published values could be found.

Two distances are listed for most stars in Table 1. The first, d_{sp}, is a spectroscopic parallax estimate based upon the MK spectral classification, observed photometric colors, and the standard reddening relation $A_V = 3.1E(B–V)$. The intrinsic OB star colors listed by Johnson (1963) and the absolute magnitudes given by Walborn (1972, 1973) for stars earlier than B3 and Blaauw (1963) for stars later than B3 were adopted. These distances have typical uncertainties of $\approx$25%, but in cases where the MK type or photometry is less certain, the errors may be larger. The second distance in Table 1, d_{tp}, is a trigonometric parallax distance based on Hipparcos data (Perryman *et al.* 1997).

The locations of the stars, as well as the location of the Vela pulsar (marked with an "X"), are shown in Figure 1. The various symbols indicate the presence or absence of high velocity Ca II absorption towards each star. In the bottom panel, Figure 1b, the locations of stars are superimposed on an IRAS 100μm image of the Vela SNR which indicates the location of dust emission in this region. The white areas indicate strong emission, with the darker shades of gray showing where such emission is weaker. The patchiness of dust in the remnant is evident in this infrared map. Additionally, a ROSAT 0.75 keV X-ray contour (Snowden *et al.* 1995) arising from the extreme edge of the adiabatically expanding shock that encircles the remnant is overplotted in white, as is a circle indicating the location of RX J0852.0–46.22, a recently discovered SNR (Aschenbach 1998).

3. DATA REDUCTION

In addition to the science spectra obtained for each of the stars in our program, multiple bias exposures, internal quartz lamp flat-field exposures, and thorium-argon arc wavelength calibration exposures were obtained. The exceptional stability of the CES resulted in reproducible calibration exposures throughout each night, as well as from night to night for identical grating positions. "Ghosts" from scattered light caused by scratches on the CES echelle grating were carefully avoided. Standard methods of bias and background subtraction and flat-fielding, were employed, all of which are described in detail by Sembach, Danks, & Savage (1993).

Thorium-argon spectra were used to convert pixel locations to wavelengths. At least 20 emission lines per wavelength region were visually identified and wavelengths were assigned to their centroids using the Th-Ar line list by Willmarth (1987). The centroids were established to an accuracy of $\pm$0.1 pixel. A second order polynomial was fit to the wavelengths of the identified lines as a function of pixel number. The RMS variations in the absolute wavelength solutions were 0.009Å or 0.66 km s^{-1} in the blue (Ca II) and 0.003Å or 0.17 km s^{-1} in the red (Na I). The FWHM of the thorium lines yielded instrumental resolutions of 4.4 km s^{-1} for the 1993–1994 data and 3.9 km s^{-1} for the 1996 data.

Many absorption line features appear in the Na I spectral region that are due primarily to water molecules within the atmosphere of the Earth. To remove these telluric features, the bright, nearby star δ Vel was observed (V = 1.96, A1 V, d = 23 pc; Hoffleit & Jaschek 1982), since it has a large $v\,sin\,i$ ($\approx$40 km s^{-1}) and minimal interstellar absorption. The spectrum of δ Vel served as a template for water line removal. The spectrum of δ Vel was fit with a cubic spline function and normalized. The atmospheric absorption lines in the spectrum of δ Vel were scaled by multiplying the optical depth of the telluric lines by a factor such that the strength of the lines from the δ Vel spectrum best matched the strength of the lines in each object spectrum at wavelengths of 5883–5901Å. The object spectra were then divided by the normalized, scaled template spectra to visibly null the Earth's atmospheric absorption features.

The observed spectra were referenced to the Local Standard of Rest (LSR) frame as defined by Mihalas & Binney (1981). This convention assigns the Sun a velocity of 16.5 km s^{-1} in the direction $l = 53°$, $b = +25°$. Earth orbital velocity corrections were calculated to an accuracy of < 0.01 km s^{-1} using a version of an algorithm originally developed by Gordon (1974). The average LSR-to-heliocentric velocity conversion value for the data set is $\Delta V_{LSR} \approx -13.1$ km s^{-1}, where $V_{LSR} = V_{helio} + \Delta V_{LSR}$.

Once all of the spectra were assigned velocities, one spectrum for each object was identified as a template and the remaining spectra of the same species were interpolated onto the same velocity grid. The spectra of each object and each epoch of observation were then summed. Since the spectra for each object were usually obtained consecutively, the differences in the velocity scales were much smaller than the velocity resolution of the data.

Each spectrum was normalized by fitting a low order ($\leq$3) polynomial to continuum regions near the interstellar absorption. Equivalent widths and errors were calculated in the standard manner. For each line, Gaussian components were fit according to the prescription outlined by Sembach *et al.* (1993). In all cases we adopted the conservative approach of fitting the fewest number of components necessary to produce a statistically meaningful description of the profiles (ie., $\chi^2_\nu \lesssim 1$). Measurement errors were propagated through the fitting process (see §5).

4. THE NEIGHBORHOOD OF THE VELA SNR

To more fully understand the complexity of the Vela SNR sight lines, the larger astronomical neighborhood of the remnant must be considered. A schematic diagram containing the Vela SNR and other prominent structures is shown in Figure 2. Our spectroscopic study probes stars in front of, within, and behind the Vela SNR.

Two other SNRs are near the Vela SNR, Puppis A (d = 2.2 kpc) centered at (l = 260°, b = −2°) (Dubner & Arnal 1988; Reynoso *et al.* 1995), and RX J0852.0–46.22 (d ∼ 200 pc) centered on (l = 266.3°, b = −1.2°) (Aschenbach 1998; Iyudin *et al.* 1998). Given the collection of SNRs, it follows that there must also be stellar associations in this general direction to provide suitable supernova candidates. Indeed, the immediate vicinity boasts several such groupings including: Vela OB1, Vela OB2, Vela R2, and Trumpler 10. Vela OB1 is centered at (l = 265°, b = −1°) at a distance of ∼1.5 kpc (Sahu 1992), while Vela R2 is located at (l = 264.5°, b = −1.5°) and d ∼ 800 pc (Herbst 1975). Using Hipparcos parallax data combined with radial velocity and photometric information, Vel OB2 (l = 263°, b = −7°); diameter ∼ 10°) and Tr 10 (l = 263°, b = 0.6°); diameter ∼ 14′) have been determined to be at distances of 410±12 pc and 366±23 pc, respectively (de Zeeuw *et al.*, 1999).

Along the Galactic equator stretches the Vela Molecular Ridge (VMR) (d ∼ 1−2 kpc). The VMR is a group of four warm giant molecular clouds that was first identified by its strong CO emission. Lending further interest to the VMR is the possibility that it is associated with the spiral arms of the Galaxy, either as a bridge between the Local and Carina arms, or as an extension of the Local arm towards the Carina arm (May, Murphy, & Thaddeus 1988; Murphy & May 1991).

Just beneath the equator, overlapping the southern edge of the VMR, is the IRAS Vela Shell. The IRAS Vela Shell is a gas and dust envelope surrounding the Vela OB2 association, centered on one of its member stars, γ^2 Velorum at (l = 263°, b = −7°). It was probably created by the combined effects of supernovae and stellar winds (Sahu 1992).

The largest feature in the Vela region is the Gum Nebula. It is an extended Hα emission source with an angular diameter of 36°, centered on (l = 258°, b = −2°). The distance to the center of the Gum Nebula is 800 pc – equal to the distance to the R association, Vela R2 (Herbst 1975; Sahu 1992). The origin of the Gum Nebula is undetermined, but current theories suggest that it could be an evolved H II region, an interstellar bubble produced by the stellar winds of OB stars, a fossil Strömgren sphere, or an extremely old SNR. (See Franco (1990) or Sahu (1992) for details on the four possibilities.)

The proximity of such a multitude of structures combines to produce a complicated montage. Certainly some structures, such as certain stellar associations and the VMR, are distant – beyond 1 kpc. The Vela SNR, IRAS Vela Shell, Gum Nebula, and RX J0852.0–46.22 all have estimated distances of ∼200–800 pc. Future studies of the Vela region will hopefully disentangle the structures, document how and if any of them are interacting, and provide a definitive atlas of the area.

Knowing the neighboring structures towards Vela, we now turn attention to the ISM that lies between the Sun and the remnant. The sight lines first penetrate nearby gas in the Local Bubble, an irregularly shaped region characterized by low-density, hot, ionized gas extending out to a radius of ∼50–70 pc (Cox & Reynolds 1987; Welsh *et al.* 1998). Extending beyond the Local Bubble, out to ∼200 pc, Ca II absorption spectroscopy reveals clouds in the local interstellar medium (LISM) that have been detected with mean LSR velocities of 0.9±9.4 km s^{-1} (Vallerga *et al.* 1993). Along southern hemisphere sight lines (Sco-Cen-Vel), LISM absorption components have been documented at velocities of −20 to +6 km s^{-1} (Crawford 1991; Welsh, Crifo, & Lallement 1998; Génova *et al.* 1997). Na I spectra towards 11 stars with distances of 100–200 pc, projected on the sky to within 15° of the SNR, reveal absorption features with -1 km s^{-1} $\lesssim V_{LSR} \lesssim$ +10 km s^{-1} (Cha *et al.*, 1999). Beyond 200 pc, many of our sight lines encounter the accelerated and compressed clouds arising from the expansion of the Vela SNR.

5. CA II AND NA I SPECTRA TOWARDS THE VELA SNR

The interstellar spectra of stars in the direction of the Vela SNR range from very simple, with only a few components, to complex, with many absorption features. The presence of many O and B stars in front of, within, and behind the remnant allows for the determination of where along the line of sight certain components arise. For instance, Ca II spectral features observed at moderate to high velocities stem from absorption by fast moving gas associated with the Vela SNR. Absorption components at low velocities are more likely caused by non-remnant foreground gas.

In Figure 3 we present the highest signal-to-noise Ca II and Na I spectra acquired for each sight line in order

of increasing HD number. Noted on each plot are the name, distance of the star, and the LSR-to-heliocentric velocity conversion factorΔV_{LSR} (see §3). The spectra of HD 72089, HD 72997, HD 73658, and HD 74455, HD 75309, and HD 75821 are discussed in §6, where evidence of time variability is presented. The spectra of the binary star HD 72127 are also omitted from Figure 3 and are discussed in §6.

In the literature, there are Ca II and Na I spectral data for some of the stars in our sample. A compilation of previously published LSR velocity and equivalent width measurements for both Ca II and Na I may be found in Tables 2 and 3 alongside new measurements. In the first column of Table 2, the star name is listed. The next four columns contain information pertaining to observations found in the literature, including: the year of observation, the central LSR velocity, the equivalent width for each absorption line identified, a reference and an indication of the type of detector used for the observation. In cases where the exact year of observation could not be determined, a range of possible dates is given. All historical velocities were first converted to the heliocentric reference frame and then corrected to the LSR defined in §3.

Columns 6–11 contain information based upon our data; observations from 1993 and 1994 are grouped in columns 6–8 while observations from 1996 are in columns 9–11. Broad absorption features, classified as lines fit with Doppler parameters of 20 $\mathrm{km\,s^{-1}} \lesssim b \lesssim 60\ \mathrm{km\,s^{-1}}$, are indicated by a superscript star (*) or filled circle ($^\bullet$) following the equivalent width measurement. If the broad feature is centered at the radial velocity of the star, a star (*) superscript is used to denote probable stellar absorption. Other broad absorption lines are flagged by a superscript filled circle ($^\bullet$) symbol and arise due to broad or unresolved interstellar absorption. Components grouped on the same horizontal line in the table indicate that the absorption detected at multiple epochs probably arose from the same gas. It was assumed that absorption features originated from the same gas if the measured velocities of the lines were within 6 $\mathrm{km\,s^{-1}}$ of each other, and if the equivalent widths of the lines were of the same order of magnitude. Some ambiguity arises from the fact that our spectra resolve more components than previously recorded in some cases.

Table 3, which contains new and historical Na I absorption line data, is organized similarly to Table 2. In Table 3, however, two equivalent widths are listed for each dataset: one for each line of the doublet (D_2, D_1). Each central LSR velocity listed is the average velocity of the D_2 and D_1 lines.

When comparing entries for a particular star in Tables 2 and 3, it is important to keep in mind that apparent variability in the absorption line data may in some cases reflect different instrumental capabilities (including whether a photographic plate or CCD was used) and different data reduction techniques. The resolution of our new data is superior to that of most previous absorption line studies of the Vela SNR, which therefore may explain the presence of components (especially weak ones) in our data set that had not been reported previously. The equivalent width errors for our data are based upon the statistical uncertainties associated with Poisson noise fluctuations and are appropriate for the assumed velocity model fit to the data. They do not account for systematic errors in continuum placement or background zero-level offsets. Both of these effects are expected to be small ($\lesssim$2%) in these data. The limits quoted in Tables 2-3 are 1σ estimates of the statistical errors.

6. TIME VARIABILITY OF INTERSTELLAR CA II AND NA I LINES

The temporal variability of absorption lines in the Vela SNR reveals the presence of rapid (t $\sim$ few years) evolution and/or motion of material within the remnant. Variability of high velocity ($|\ V_{LSR}\ | > 50\ \mathrm{km\,s^{-1}}$) absorption lines is apparent in five stars, while two stars exhibit changes at lower velocities. The low incidence of detectable variability in low velocity absorption lines may be a selection effect since in most spectra there are simply too many absorption lines blended together at low velocity to observe slight differences in the characteristics of individual components. Excluding Vela sight lines, there is only one other convincing case of temporal variability of an optical absorption line. Blades *et al.* (1997, see also Blades & Penprase 1999) report variability in gas at $|V_{LSR}| < 30$ $\mathrm{km\,s^{-1}}$ toward HD 28497, ($l = 208.78°$, $b = -37.40°$).

In Figures 4–10, we highlight spectra of the sight lines towards HD 72089, HD 72127, HD 72997, HD 73658, HD 74455, HD 75309, and HD 75821, which have detectable changes in the column density of Ca II and/or Na I absorption lines and/or shifts in the central velocities of the lines. Details pertaining to possible physical explanations for the variations are discussed below. The measured velocities, V_{LSR}, column densities, N, equivalent widths, W_λ, and the LSR-to-heliocentric velocity conversion factors, ΔV_{LSR}, of the variable lines are summarized in Table 4.

6.1. *HD 72089*

The Na I D lines of HD 72089 (Figure 4) contain a component at $V_{LSR} \approx +105\ \mathrm{km\,s^{-1}}$ whose equivalent width decreased by ∼60% from 1993 to 1996. Analysis of the Ca II line at the same velocity shows a decrease in its equivalent width of ∼17% during the same period of time. Since the amount of Ca II decreased more slowly than Na I, the ratio of the column densities of Ca II to Na I increased by more than twofold: in 1993 N(Ca II)/N(Na I) = 3.4, while in 1996 N(Ca II)/N(Na I) = 7.2. An increase in the number of ionizing photons in the $+105\ \mathrm{km\,s^{-1}}$ gas could cause the observed metamorphosis of the Ca II and Na I lines given that the ionization potentials (IP) of these two ions are 11.87 eV and 5.14 eV, respectively.

6.2. *HD 72127*

We obtained Ca II absorption line spectra towards HD 72127A in 1994 and 1996, and towards HD 72127B, a binary companion, in 1996 (Figure 5). Comparison of the Ca II spectra of HD 72127A and B reveals immediately that the $V_{LSR} \approx 0\ \mathrm{km\,s^{-1}}$ component of HD 72127B has an equivalent width twice that of HD 72127A. This dominant feature in the spectrum of HD 72127B is probably a blend of absorption lines at $V_{LSR} \approx -10$ and $+1$ $\mathrm{km\,s^{-1}}$. A higher resolution spectrum of HD 72127B with these two lines resolved could reveal details about the small

scale structure in the Vela region. There may be interstellar density inhomogeneities in the slightly separated sight lines towards HD 72127A and B, or perhaps the sight line towards HD 72127B penetrates an additional low velocity cloud that HD 72127A does not. The two stars are 2500 AU apart (Thackeray 1974), separated by more than enough distance for there to be variations in the structure of the ISM through which their sight lines pass. It has been documented that there exists small scale structure in the interstellar medium revealed by the comparison of the stars in the binary system μ Cru at a separation of 6600 AU (Meyer & Blades 1996), and across distances as small as 5–100 AU using unrelated background sources (Frail *et al.* 1994). Interestingly, no subsequent variations in Na I line intensity have been observed toward μ Cru over a recent 21 month baseline (Lauroesch *et al.* 1998).

Absorption along the sight line towards HD 72127A varies with time. Analysis of our Ca II spectra of HD 72127A from 1994 and 1996, reveals that the relative intensities of the components at $V_{LSR} = -10$ km s^{-1} and $+1$ km s^{-1} have reversed, primarily because of the 11% decrease in equivalent width of the $V_{LSR} = -10$ km s^{-1} line. During the same epoch, the two absorption lines at $V_{LSR} = -28$ km s^{-1} and -21 km s^{-1} increased in equivalent width by ∼20%. Because these three lines are so closely spaced in velocity, it is difficult to assign a unique fit to the lines in the spectra. It is likely that the components at $V_{LSR} = -28$ km s^{-1} and -21 km s^{-1} are remnant gas, but we do not know where the -10 km s^{-1} component is located along the sight line. The Ca II gas concentration towards HD 72127A has indeed changed between 1994 and 1996, but the blended lines result in some ambiguity in making a quantitative measurement of the variability.

The variable nature of the column densities associated with the clouds towards HD 72127A has been documented by Hobbs *et al.* (1991) also. Looking at eight Ca II spectra that Hobbs *et al.* obtained from November 1981 through December 1988, the $V_{LSR} \approx -10$ km s^{-1} component is clearly stronger than the $V_{LSR} \approx +1$ km s^{-1} component (which they identify as a blend of two lines) from November 1982 through November 1986, then vice versa in December 1988. As they documented in the long time series of data they presented, the strengths of both the $V_{LSR} \approx -10$ and $+1$ km s^{-1} lines change over time as do the radial velocities of both absorption lines. Neither our data, nor the Hobbs *et al.* data contain evidence of a cyclic pattern to the changes.

The Hobbs *et al.* Na I spectra of HD 72127A also clearly exhibit variable column densities in the lines at $V_{LSR} \approx -10$ and $+1$ km s^{-1}. Since we obtained a spectrum of HD 72127A in 1994 only, we cannot confirm the presence of recent variability of this ion in the high velocity gas of the Vela SNR.

6.3. *HD 72997*

Figure 6 depicts the evolution of Ca II and Na I absorption lines toward HD 72997 at three epochs. These plots clearly show shifts in the central line velocity of both species near $V_{LSR} \approx +190$ km s^{-1} first reported by Danks & Sembach (1995). We reproduce their 1991 and 1993 spectra here, and add new spectra from 1996. The line at $V_{LSR} \approx +190$ km s^{-1} appears to be continuing its shift towards a larger positive velocity. From 1991 to 1993, $\Delta V = 2.7$ km s^{-1} for the high velocity Na I data and $\Delta V = 1.4$ km s^{-1} for the Ca II data. Examining the epoch 1993 to 1996 we find $\Delta V = 1.1$ km s^{-1} and $\Delta V = 0.9$ km s^{-1} for the Na I and Ca II data respectively, leading to total shifts of $\Delta V = 3.8$ km s^{-1} for the high velocity Na I component and $\Delta V = 2.3$ km s^{-1} for the Ca II component over five years. Such changes indicate that on average, that the acceleration of this high velocity gas is decreasing with time. The acceleration does not appear to have caused a net change in the equivalent width of either Ca II or Na I over the five-year period.

6.4. *HD 73658*

The intermediate velocity features at ∼-32 km s^{-1} and -15 km s^{-1} in the Ca II spectrum of HD 73658 decreased dramatically between observations in 1993 and 1996. The equivalent width of the ∼-32 km s^{-1} line decreased from 41±1 mÅ to 4±2 mÅ, a 90% reduction, while the -15 km s^{-1} line decreased by 53%. The Ca II spectra from both observations are plotted together and shown in the left panel of Figure 7. Although the column density of intermediate negative velocity gas in this spectrum diminished since 1993, neither the high velocity absorption component at ∼-127 km s^{-1} nor the low and intermediate positive velocity components changed during the same time period. The gas at ∼-32 km s^{-1} and -15 km s^{-1} is probably patchy, with a dense region probed by the sight line in the 1993 observation and a less dense region penetrated in 1996. The Na I D_2 spectrum of HD 73658 is shown in the right panel of Figure 7, as observed in both 1993 and 1996, yet there is no evidence of time variability and there are no absorption features at intermediate negative velocities.

6.5. *HD 74455*

The high velocity feature at $V_{LSR} = -173$ km s^{-1} in the Ca II spectrum of HD 74455 decreases in equivalent width by 28% from 1994 to 1996. There is no change of this magnitude in any of the other absorption components in the Ca II spectrum or in the Na I spectrum. Figure 8 illustrates that the Na I spectrum does not contain absorption at high velocities, although the low – intermediate velocity profile is similar to that of Ca II. The equivalent width decrease at -173 km s^{-1} suggests that the amount of high velocity low ionization gas along the sight line has diminished. The sight line towards HD 74455 probes a different piece of the -173 km s^{-1} gas packet in 1996 than it did in 1993. It does not appear that the reduction in column density is due to the acceleration/deceleration of some of the gas since the equivalent widths of the two absorption features flanking the -173 km s^{-1} line do not vary (see Table 2).

6.6. *HD 75309*

In the Ca II spectrum of HD 75309 shown in Figure 9, we note three line components that have changed between observations in 1993 and 1996. First, the absorption feature at $V_{LSR} \approx -119$ km s^{-1} has increased in equivalent width by 25%. Second, in the 1993 spectrum, two absorption features are present at $V_{LSR} = +81$ km s^{-1} and $+89$ km s^{-1}, with equivalent widths of 4 mÅ and 7 mÅ, respectively; these lines are not detected in the 1996 spectrum.

The variable absorption feature at -119 km s^{-1} could result from one or both of the following mechanisms: the continuing compression of a patch of high velocity gas, or the liberation of Ca II due to grain destruction at high velocities (Spitzer 1978). We do not detect this high velocity absorption line in the Na I spectrum, nor do we see any intermediate velocity Na I absorption corresponding to the rather complicated Ca II spectrum.

We do not detect the pair of Ca II absorption lines found in the 1993 spectrum at $V_{LSR} = +81$ km s^{-1} and $+89$ km s^{-1} in the 1996 repeat observation. The non-detection allows us to place an upper limit on the equivalent widths of < 3 mÅ (3σ) in the 1996 spectrum. With only two observations of HD 75309, we are not able to determine whether these features were present for a long time and suddenly disappeared, or whether the lines were ephemeral. Since the 1996 spectrum shows no trace of Ca II at these velocities, the most likely interpretation of the presence and subsequent absence of these absorption features is that a wisp of gas containing a column density of N(Ca II) $\approx 5 \times 10^{10}$ cm^{-2} temporarily passed across the sight line.

6.7. *HD 75821*

Our 1993 and 1996 Ca II and Na I spectra of HD 75821 are displayed in Figure 10. The plots on the right side of Figure 10 magnify a pair of spectral lines whose equivalent widths have changed between the two observations. The central velocity of one component is also changing.

The equivalent width of the Ca II absorption line at $V_{LSR} = -85$ km s^{-1} decreased by $\sim$20% while the Na I lines associated with absorption by the same gas decreased by $\sim$50%. This results in an increase in the Ca II to Na I ratio of $\sim$40%, which is likely to occur in a region experiencing dust destruction (Spitzer 1978). See Danks & Sembach (1995) for a summary of recent work focusing on shock models and their implications for gas phase abundances in SNR gas.

The Ca II and Na I absorption features apparent near -99 km s^{-1} increased in equivalent width by $\sim$20% from one observation epoch to the next. In addition, both lines exhibit increased central velocities in 1996: for Ca II $\Delta V = 1.43 \pm 0.10$ km s^{-1} and for Na I $\Delta V = 1.43 \pm 0.45$ km s^{-1}. The increase in column density of both ions coupled with the increasing velocity of the spectral line suggests that the high velocity gas is being accelerated.

Not only does the sight line towards HD 75821 reveal two pockets of gas whose physical characteristics vary on short timescales, these spectra are unusual in another way: they serve as a counterexample to the "Routly-Spitzer effect". In 1993 (1996), the ratio N(Ca II)/N(Na I) is $\sim$5 (12) times higher for the lower velocity line at $V_{LSR} \approx -85$ km s^{-1} than for the line at $V_{LSR} \approx -99$ km s^{-1}, while the observational trend described by Routly & Spitzer (1952) states that the ratio should increase with increasing velocity.

7. DISCUSSION

Multiple spectroscopic observations of a large sample of O and B stars in the direction of the Vela SNR have enabled us to confirm and extend the reports of short timescale changes in the spectra of the stars HD 72089, HD 72997, and HD 72127, as well as discover variability in the spectra of HD 73658, HD 74455, HD 75309 and HD 75821. Many of the cases of variability have occured in spectral lines at high velocities, indicating that the changes in the absorption profiles are due to the evolving SNR. Thirteen stars were observed at two epochs. Of these, three were known to exhibit variability. Eliminating these stars, four of ten randomly chosen sight lines revealed variability. The sample is too small to confidently state the probability of observing variability, but if more stars were observed at an additional epoch, the nature of variability in the remnant could be explored in greater detail. If a large percentage of spectra changed over time, one could conclude that 1) changing conditions persist over "long" time periods and/or 2) changing conditions are ubiquitous in the remnant. On the other hand, if a small fraction of the spectra observed changed over time, the conclusions that could be reached include 1) changing conditions are short lived (less than a few years) and/or 2) variability along sight lines through the Vela SNR is rare.

We note that there has been a recent discovery of an X-ray bright supernova remnant (RX J0852.0-4622) in the direction of Vela (Aschenbach 1998). Both the X-ray and γ-ray emissions from this object indicate that it is within 1 kpc of the Sun, and perhaps as close as 200 pc (Aschenbach 1998; Iyudin *et al.* 1998). If the remnant lies as close as 200 pc, then it is possible that RX J0852.0$-$4622 and the Vela SNR are physically related. One of our sight lines, HD 75821, passes very near to RX J0852.0$-$4622. The sight line contains high velocity gas, but there is nothing peculiar about the optical absorption properties compared to those of other high velocity gas features toward other Vela stars.

An extensive study of Ca II and Na I in high velocity gas over a period of time may provide insight into the dynamics and evolution of the Vela SNR since the absorption properties of numerous sight lines through the remnant appear to be changing over time periods of several years. We hope that the compilation of spectroscopic data in this paper will be useful for tracking the development and evolution of absorption lines traversing the SNR. Studies of dominant ionization stages along some of these same sight lines with the Hubble Space Telescope would be useful for studying the changing physical conditions. In addition, repeat observations separated by a few months, and others spaced by $\sim$5 years would allow the timescale of the changes to be determined more accurately, resulting in a more thorough understanding of the evolution of the Vela SNR gas.

It would also be desirable to monitor the spectra of a modest sample of stars outside the Vela region to determine if variability is common in the diffuse ISM. Evidence of variability in such regions could have a substantial impact on studies relying on comparisons of data taken at different epochs.

We thank Anthony Danks for his assistance with the observations. We appreciate comments on this work from our colleagues in the Department of Physics and Astronomy at the Johns Hopkins University. We acknowledge use of the Simbad Database at the Centre Données astronomiques de Strasbourg (http://simbad.u-strasbg.fr/Simbad), and use of the NASA SkyView facility located at the Goddard Space Flight Center (http://skyview.gsfc.nasa.gov).

KRS and ANC appreciate support from NASA Long Term Space Astrophysics Grant NAG5-3485 and grant GO-06413-95A from the Space Telescope Science Institute, which is operated by AURA under NASA contract NAS5-26555.

REFERENCES

Aschenbach, B. 1993, AdSpR, 13, 45
Aschenbach, B. 1998, Nature, 396, 141
Blades, J.C. & Penprase, B. 1999, in preparation
Blades, J.C., Sahu, M.S., He, L., Crawford, I.A., Barlow, M.J., & Diego, F. 1997, ApJ, 478, 648
Blaauw, A. 1963, in *Basic Atronomical Data*, K.A. Strand, Ed. (U. of Chicago Press, Chicago)
Buscombe, W. 1969, MNRAS, 144, 31
Cha, A.N., Sahu, M.S., Moos, H.W., Blaauw, A., 1999, in preparation
Cha, A.N., Sembach, K.R., & Danks, A.C. 1999, ApJ, 515, L25 (Paper I)
Corbally, C.J. 1984, ApJS, 55, 657
Cousins, A.W.J. 1972, MNASSA, 31, 75
Cousins, A.W.J. & Stoy, R.H. 1962, R. Obs. Bull., 64
Cox, D.P. & Reynolds 1987, ARA&A, 25, 303
Crampton, D. 1971, AJ, 76, 260
Crawford, I.A. 1991, A&A, 247, 183
Danks, A. & Sembach, K. 1995, AJ, 109, 2627
Dekker, H., Delabre, B., D'Odorico, S., Lindgren, H., Maaswinkel, F., & Reiss, R. 1986, The Messenger, 43, 27
Denoyelle, J. 1977, A&AS, 27, 343
Denoyelle, J. 1987, A&AS, 70, 373
Deutschman, W.A., Davis, R.J., & Schild, R.E. 1976, ApJS, 30, 97
de Zeeuw, P.T., Hoogerwerf, R., de Bruijne, J.H.J., Brown, A.G.A., & Blaauw, A. 1999, AJ, 117, 354
Dubner, G.M. & Arnal, E.M. 1988, A&AS, 75,363
Evans, D.S. 1979, IAU Symp. 30, 57
Feast, M.W., Stoy, R.H., Thackeray, A.D., & Wesselink, A.J. 1961, MNRAS, 122, 239
Feast, M.W., Thackeray, A.D. & Wesselink, A.J. 1955, MemRAS, 67, 51
Frail, D.A., Weisberg, J.M., Cordes, J.M., & Mathers, C. 1994, ApJ, 436, 144
Franco, G.A.P. 1990, A&A, 227, 499
Garrison, R.F., Hiltner, W.A., & Schild, R.E. 1977, ApJS, 35, 111
Génova, R., Beckman, J., Bowyer, S., & Spicer, T. 1997, ApJ, 484, 761
Gordon, M.A. 1974, in *Methods of Experimental Physics*, Volume 12, edited by M.L. Meeks (Academic Press: New York), Chap. 6.1
Herbst, W. 1975, AJ, 80, 683
Hiltner, W.A., Garrison, R.E., & Schild, R.E. 1969, ApJ, 157, 313
Hobbs, L.M., Ferlet, R., Welty, D.E., & Wallerstein, G. 1991, ApJ, 378, 586
Hoffleit, D. & Jasckek, C. 1982, *The Bright Star Catalog* (Yale University Observatory: New Haven)
Houk, N. 1978, *Michigan Spectral Survey*, Ann Arbor, Department of Astronomy, University of Michigan
Iyudin, A.F., Schönfelder, V., Bennett, K., Bloemen, H., Diehl, R., *et al.* 1998, Nature, 396, 142
Jenkins, E.B., Wallerstein, G., & Silk, J. 1984, ApJ, 278, 649
Johnson, H.L. 1963, in *Basic Astronomical Data*, K.A. Strand, Ed. (U. of Chicago Press, Chicago), p.214
Johnson, H.L., Iriarte, B., Mitchell, R.I., & Wisniewski, W.Z. 1966, Comm. Lunar Plan. Lab., 4, 99
Kaper, L. & Pasquini, L. 1996, *The Coudé Auxiliary Telescope / Coudé Echelle Spectrometer Operating Manual*, CAT-MAN-0633-0001, European Southern Observatory
Lauroesch, J.T., Meyer, D.M., Watson, J.K., & Blades, J.C. 1998, ApJ, 507, L89
Loden, L.O. 1968, Ark. Astr., 4, 425
May, J., Murphy, D.C., & Thaddeus, P. 1988, A&AS, 73, 51
Meyer, D.M. & Blades, J.C. 1996, ApJ, 464, L179
Mihalas, D. & Binney, J. 1981, *Galactic Astronomy*, (W. H. Freeman and Co.: New York), Chap. 6
Moffat, A.F.J. & Vogt, N. 1975, A&AS, 20, 85
Morris, P.M. 1961, MNRAS, 122, 325
Murphy, D.C. & May, J. 1991, A&A, 247, 202
Perryman, M.A.C., Lindegren, L., Kovalevsky, J., Hog, E., Bastian, U., *et al.* 1997, A&A, 323, L49
Reichley, P.E., Downs, G.S., & Morris, G.A. 1970, ApJ, 159, L35
Reynoso, E.M., Dubner, G.M., Goss, W.M., & Arnal, E.M. 1995, AJ, 110, 318
Roman, N.G. 1978, AJ, 83, 172
Routly, P.M. & Spitzer, L. 1952, ApJ, 115, 227
Sahu, M.S. 1992, Ph.D. Thesis, University of Groningen
Schild, R.E., Garrison, R.E., & Hiltner, W.A. 1983, ApJS, 51, 321
Sembach, K.R., Danks, A.C., & Savage, B.D. 1993, A&AS, 100, 107
Snowden, S.L., Freyberg, M.J., Plucinsky, P.P., Schmitt, J.H.M.M., Truemper, J., *et al.* 1995, ApJ, 454, 643
Spitzer, L. 1978, *Physical Processes in the Interstellar Medium*, (Wiley-Interscience: New York)
Thackeray, A.D. 1974, Observatory, 94, 55
Thackeray, A.D. & Andrews, P.J. 1974, A&AS, 16, 323
Thackeray, A.D., Tritton, S.B., & Walker, E.N. 1973, MemRAS, 77, 1977
Thackeray, A.D., & Warren, P.R. 1972, MNRAS, 160, 23P
Uesugi A. & Fukuda I. 1982, *Revised Catalogue of Stellar Rotational Velocities*, Department of Astronomy, Kyoto University
Vallerga, J. V., Vedder, P. W., Craig, N., & Welsh, B. Y. 1993, ApJ, 411,729
Walborn, N.R. 1972, AJ, 77, 312
Walborn, N.R. 1973, AJ, 78, 1067
Wallerstein, G. & Silk, J. 1971, ApJ, 170, 289
Wallerstein, G., Silk, J., & Jenkins, E.B. 1980, ApJ, 240, 834
Wallerstein, G. & Gilroy, K.K. 1992, AJ, 103, 1346
Welsh, B.Y., Craig, N., Vedder, P.W., & Vallerga, J.V. 1994, 437, 638
Welsh, B.Y., Crifo, F., & Lallement, R. 1998, A&A, 333, 101
Willmarth, D. 1987, *A CCD Atlas of Comparison Spectra: Thorium-Argon Hollow Cathode 3180Å–9540Å*, Kitt Peak National Observatory
Wilson, R.E. 1953, *General Catalogue of Stellar Radial Velocities*, (Carnegie Inst.: Washington, D.C.), Publ. 601

Figure Captions

Figure 1. A plot of the stars in our sample a) as projected onto the sky, and b) as projected onto an IRAS 100 μm image of the Vela region shown in logarithmic gray-scale. The contour shown is a ROSAT 0.75 keV contour with 4×10^{-4} counts s^{-1} $arcmin^{-2}$. Different symbols indicate the maximum velocity gas observed along a particular sight line. The circle in panel b) shows the location and size of SNR RX J0852.0–46.22.

Figure 2. A schematic diagram showing the extended structures and stellar associations present in the direction of the Vela SNR. The 'X' indicates the location of the Vela Pulsar.

Figure 3. Plots of the normalized Ca II and Na I spectra in our sample. If only a Ca II spectrum is shown for a given star, the corresponding Na I spectrum was not obtained. The LSR-to-heliocentric velocity conversion factor, ΔV_{LSR}, where $V_{LSR} = V_{helio} + \Delta V_{LSR}$, and the distance are noted at the bottom of each panel.

Figure 4. Comparisons of the Ca II and Na I spectra of HD 72089 observed in February 1993 (dotted lines) and January/February 1996 (solid lines). The left panels show the reduced, normalized spectra. The right panels provide close-up views of high velocity features that changed between our observations. Notice the dramatic decrease in the column density and displacement of the line center of the Na I line near +105 $km\,s^{-1}$.

Figure 5. Panel (a) contains the Ca II spectra towards the two components of the visual binary star, HD 72127A (solid line) and HD 72127B (dotted line). Panel (b) shows a comparison of the HD 72127A Ca II spectra obtained in 1994 (dotted line) and 1996 (solid line). Panels (c) and (d) contain the spectra of the HD 72127A Na I D_2 and D_1 lines, respectively, as observed in 1994.

Figure 6. Comparisons of the Ca II and Na I spectra of HD 72997 observed in December 1991 (gray lines), February 1993 (dotted lines) and January/February 1996 (black lines). The left panels show the reduced, normalized spectra. The right panels provide close-up views of the high velocity feature near +190 $km\,s^{-1}$ for both Ca II and Na I. Note the systematic shift of this high velocity feature towards higher velocity over the five year period.

Figure 7. The left panel shows the Ca II spectrum of HD 73658 as observed in 1993 (dotted line) and 1996 (solid line), while the right panel depicts the Na I D_2 spectrum as obtained at the same epochs. The amount of low – intermediate negative velocity Ca II gas decreased between the observations.

Figure 8. Spectra of HD 74455 are shown using dotted lines for the 1994 observations and solid lines for the 1996 observations. The upper panels exhibit Ca II absorption which varies between the observations in the high velocity component. The lower panels illustrate the Na I D_2 and D_1 line profiles which do not vary from 1994 to 1996.

Figure 9. The Ca II spectrum of HD 75309 as observed in 1993 (dotted lines) and 1996 (solid lines) is shown in panel (a). Panels (b) and (c) are close up views of two absorption line features that appear to have changed between observations. Panel (d) depicts the Na I spectrum of HD 75309 observed in 1993.

Figure 10. Comparisons of the Ca II and Na I spectra of HD 75821 observed in February 1993 (dotted lines) and January/February 1996 (solid lines). The left panels show the reduced, normalized spectra of HD 75821. The right panels provide close-up views of high velocity features that occur near −85 $km\,s^{-1}$ and −98 $km\,s^{-1}$ for Ca II and Na I, respectively. These spectra reveal time variability in the equivalent widths and velocities of the absorption features.

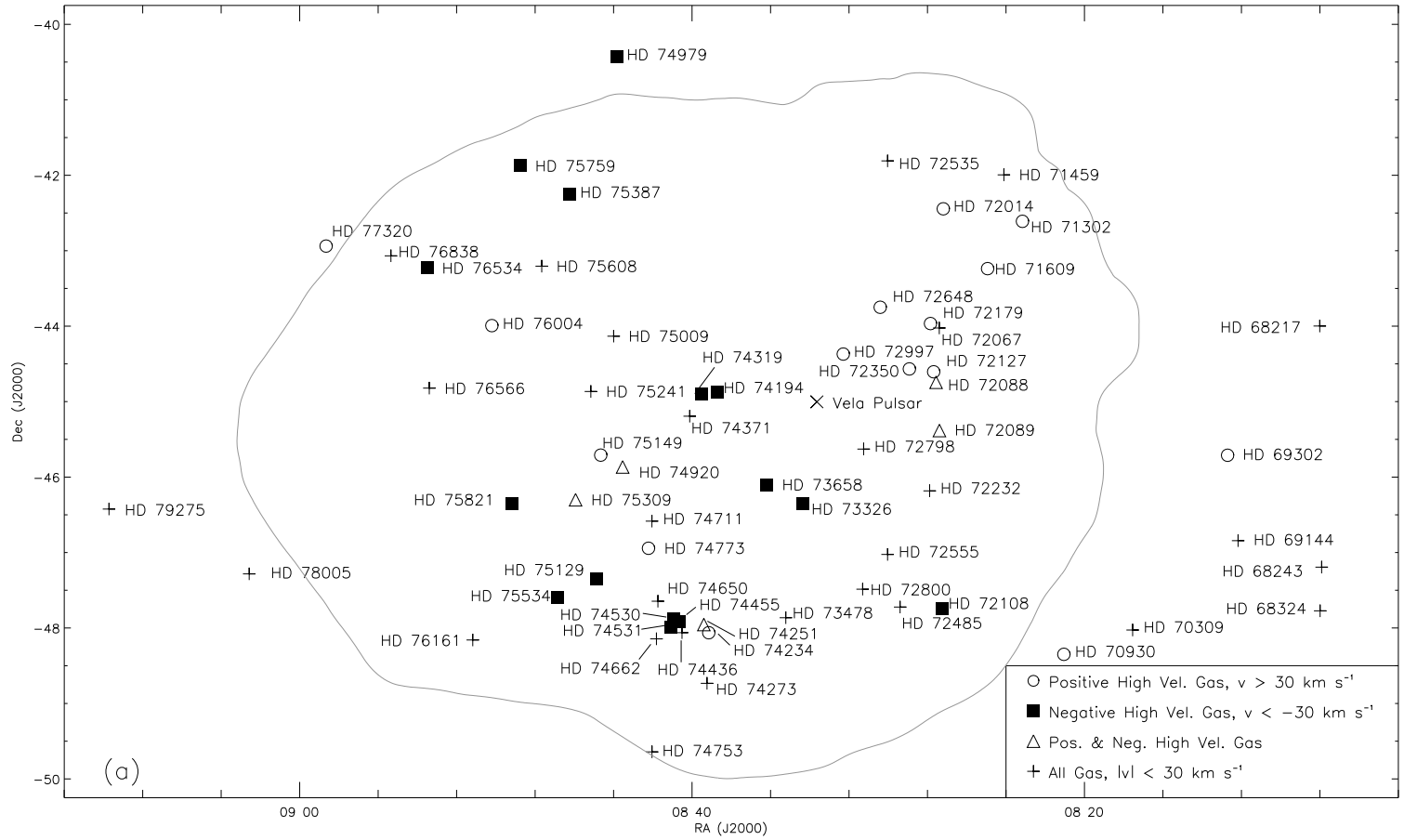
HD 74979
HD 75759
HD 75387
HD 72535
HD 71459
HD 72014
HD 71302
HD 77320
HD 76838
HD 76534
HD 75608
HD 71609
HD 72648
HD 72179
HD 76004
HD 75009
HD 68217
HD 72067
HD 74319
HD 72997
HD 72127
HD 72350
HD 76566
HD 75241
HD 74194
HD 72088
Vela Pulsar
HD 74371
HD 72089
HD 75149
HD 72798
HD 69302
HD 74920
HD 73658
HD 72232
HD 79275
HD 75821
HD 75309
HD 73326
HD 74711
HD 74773
HD 69144
HD 72555
HD 78005
HD 75129
HD 68243
HD 74650
HD 72800
HD 75534
HD 74455
HD 72108
HD 74530
HD 73478
HD 68324
HD 74531
HD 72485
HD 74251
HD 70309
HD 76161
HD 74234
HD 70930
HD 74662
HD 74436
HD 74273
HD 74753
Positive High Vel. Gas, v > 30 km s⁻¹
Negative High Vel. Gas, v < −30 km s⁻¹
Pos. & Neg. High Vel. Gas
All Gas, lvl < 30 km s⁻¹
(a)
−40
−42
−44
−46
−48
−50
Dec (J2000)
09 00
08 40
08 20
RA (J2000)

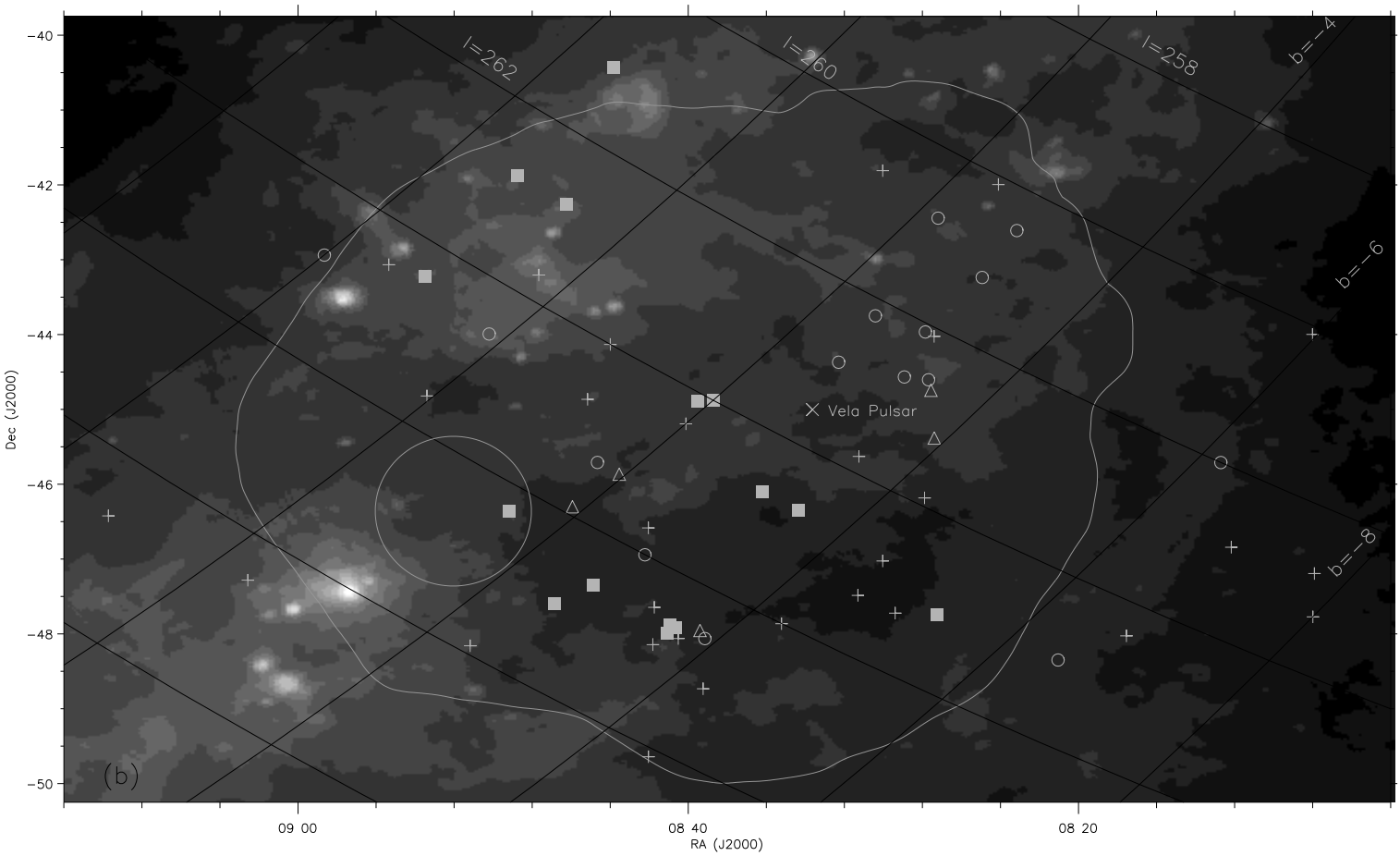
l=262
l=260
l=258
b=−4
b=−6
b=−8
Vela Pulsar
(b)
−40
−42
−44
−46
−48
−50
Dec (J2000)
09 00
08 40
08 20
RA (J2000)

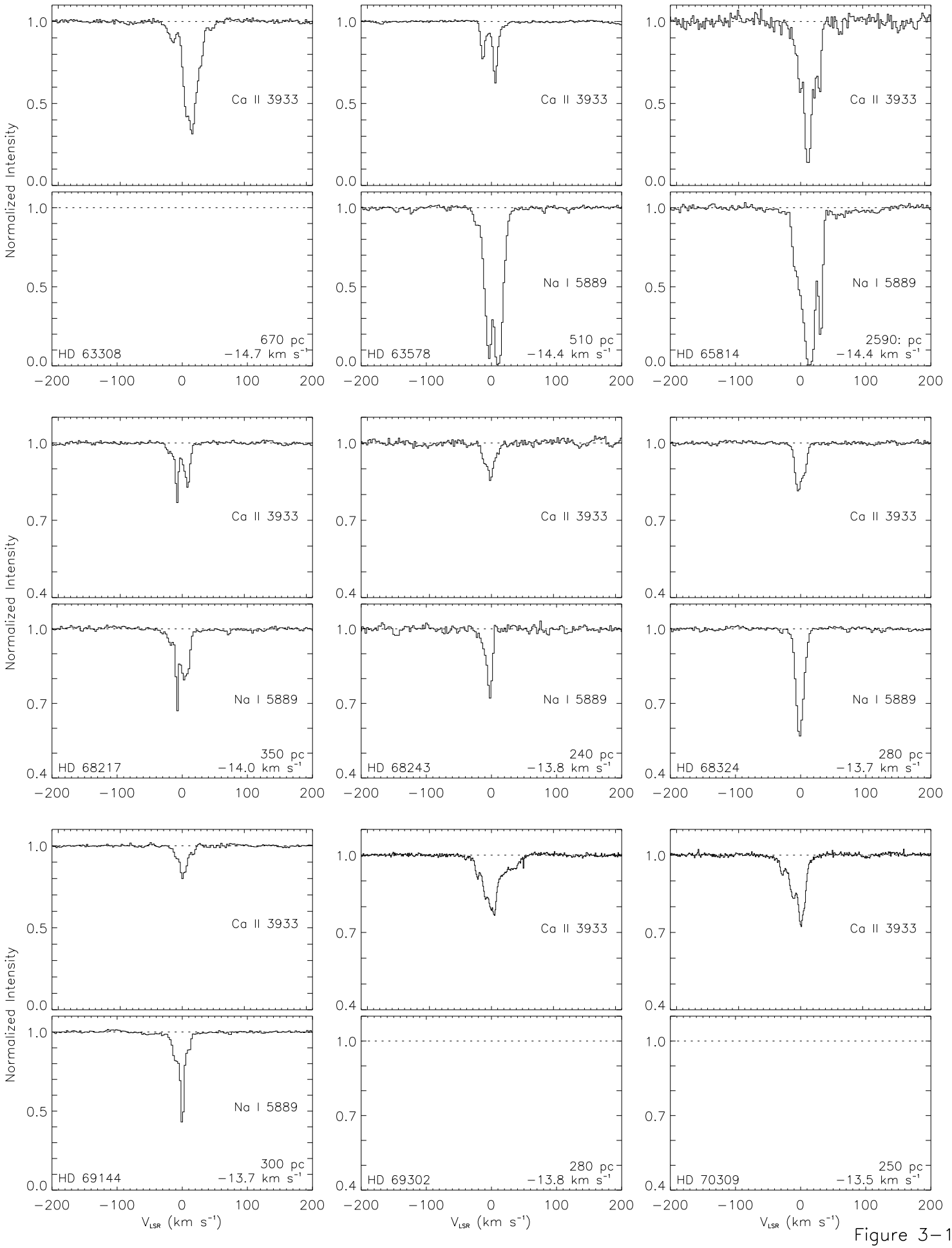
Normalized Intensity
Ca II 3933
Na I 5889
HD 63308
670 pc
−14.7 km s−1
HD 63578
510 pc
−14.4 km s−1
HD 65814
2590: pc
−14.4 km s−1
HD 68217
350 pc
−14.0 km s−1
HD 68243
240 pc
−13.8 km s−1
HD 68324
280 pc
−13.7 km s−1
HD 69144
300 pc
−13.7 km s−1
HD 69302
280 pc
−13.8 km s−1
HD 70309
250 pc
−13.5 km s−1
VLSR (km s−1)

Figure 3−1

arXiv:astro-ph/9909128v1 7 Sep 1999

TABLE 1
STELLAR INFORMATION[a]

Object	l (°)	b (°)	MK[b]	V (mag)	B–V (mag)	E_{B-V} (mag)	d_{sp}[c] (pc)	d_{tp}[d] (pc)	v_{rad}[e] ($km\,s^{-1}$)	$v\ sin\ i$ ($km\,s^{-1}$)	Refs.[f,g]
HD 63308	254.36	−7.54	B2 V	6.57	−0.13	0.11	490	700±260	+34	···	2,13
HD 63578	260.25	−10.56	B1.5 IV	5.23	−0.14	0.11	480	510±120	+34	200	6,13
HD 65814	255.79	−5.66	B2 III:	9.0:	−0.1:	0.14	2590:	···	(+30)	103	11,23
HD 68217	260.07	−5.96	B2 IV-V	5.21	−0.19	0.05	340	350±60	+8	250	3,13
HD 68243	262.81	−7.70	B1 V [v]	4.27	−0.24	0.02	240	···	+20	115	3,13
HD 68324	263.33	−7.98	B1 IVe [v]	5.23	−0.21	0.05	520	280±40	+5	245	2,13
HD 69144	262.88	−6.92	B2.5 IV [s]	5.13	−0.16	0.07	300	300±50	+25	85	1,13
HD 69302	261.98	−6.17	B2 IV-V [m]	5.84	−0.19	0.05	450	280±40	+20	···	1,12
HD 70309	264.41	−6.81	B3 V [m]	6.45	−0.14	0.06	390	250±35	+26	···	2,14
HD 70930	264.98	−6.50	B1.5 III [m]	4.82	−0.15	0.10	550	460±120	+27	220	3,13
HD 71302	260.50	−2.89	B3 V [s]	5.95	−0.15	0.05	320	950±650	+23	(179)	1,12
HD 71459	260.10	−2.40	B3 V	5.47	−0.14	0.06	250	250±30	+28	60	3,13
HD 71609	261.20	−3.01	B3 II	7.87	+0.10	0.28	2090	1270±1170	+25	···	1,12
HD 72014	260.77	−2.20	B0 Vnne [e]	6.25	−0.07	0.23	670	930±450	+5	265	1,12
HD 72067	262.08	−3.08	B2 Vn [e]	5.83	−0.16	0.08	360	490±150	+3	136	1,12
HD 72088	262.67	−3.49	B3 III-IV:	9.07	+0.03	0.23	1630:	···	(+32)	(140)	4,23
HD 72089	263.21	−3.89	B5 II-III:	7.6:	−0.1:	0.05:	1600:	···	···	(>250)	11,23
HD 72108	265.14	−5.28	B1.5 V [m]	5.53	−0.15	0.10	380	500±190	···	95	10
HD 72127A	262.57	−3.36	B2 III	5.20	−0.18	0.10	480	···	+22	210	10
HD 72127B	262.57	−3.36	B2.5 V	7.09	−0.10	0.10	480	···	···	···	10
HD 72179	262.08	−2.97	B5 V	8.14	−0.12	0.04	640	···	···	···	4,20
HD 72232	263.91	−4.26	B7 IV	5.99	−0.15	0.00	290	190±20	+12	(105)	6,19
HD 72350	262.71	−3.19	B4 IV [m]	6.30	−0.02	0.16	390	680±310	+24	(260)	1,12
HD 72485	265.30	−4.96	B2.5 V	6.38	−0.14	0.09	350	320±50	+11	(55)	1,12
HD 72535	260.64	−1.43	B2 V [m]	8.20	+0.07	0.31	770	···	···	···	7,20
HD 72555	264.84	−4.52	B2.5 V	7.03	−0.14	0.09	470	390±90	+26	175	9,15
HD 72648	262.23	−2.48	B2.5 II-III [m]	7.61	+0.12	0.34	1340	740±360	(+70)	(87)	1,12
HD 72798	263.77	−3.46	B5 III [m]	6.45	−0.14	0.02	520	750±310	+22	(55)	5,14
HD 72800	265.26	−4.57	B9 I	6.64	+0.12	0.12	2260	···	+34	75	1,14
HD 72997	262.92	−2.58	B2 V [c]	7.46	−0.18	0.06	780	620±260	(+30)	(73)	8,20
HD 73326	264.69	−3.48	B2 IV	7.27	−0.03	0.21	800	···	+49	···	1,12
HD 73478	265.96	−4.29	B3 IV:	7.37	−0.10	0.10	820:	910±500	−1	···	2,23
HD 73658	264.68	−3.13	B1 II [e]	6.86	+0.04	0.28	1580	720±280	+52	111	1,12
HD 74194	264.04	−1.95	O8.5 Ib(f) [p]	7.57	+0.21	0.50	2800	···	−4	180	1,12
HD 74234	266.56	−3.87	B2 V	6.95	−0.17	0.07	610	630±230	+27	250	5,14
HD 74251	266.45	−3.76	B3 IV-V:	7.76	−0.11	0.09	840:	650±280	−23	···	4,23
HD 74273	267.13	−4.27	B1.5 V	5.92	−0.20	0.05	490	490±120	+18	190	1,12
HD 74319	264.07	−1.80	B5 V [m]	6.69	−0.10	0.06	320	400±90	···	(170)	2,20
HD 74371	264.44	−2.01	B6 Ia [p]	5.24	+0.21	0.28	1920	830±360	+24	30	1,13
HD 74436	266.70	−3.72	B3 V: [m]	8.24	−0.08	0.12	820:	410±230	−1	···	4,23
HD 74455	266.60	−3.61	B1.5 Vn [v]	5.48	−0.17	0.08	390	520±150	+42	370	1,12
HD 74530	266.62	−3.55	B3 IV-V: [m]	8.68	−0.12	0.08	1300:	···	+3	(165)	4,23
HD 74531	266.68	−3.61	B2 III [m]	7.25	−0.16	0.08	1260	780±520	+4	(165)	1,12

TABLE 1—*Continued*

Object	l (°)	b (°)	MK[b]	V (mag)	B–V (mag)	E_{B-V} (mag)	d_{sp}[c] (pc)	d_{tp}[d] (pc)	v_{rad}[e] ($km\,s^{-1}$)	$v\ sin\ i$ ($km\,s^{-1}$)	Refs.[f,g]
HD 74650	266.47	−3.30	B9 V:	7.35	−0.05	0.01	220:	···	···	···	2,23
HD 74662	266.90	−3.63	B3 V:	8.82	−0.07	0.13	1060:	···	−13	···	2,23
HD 74711	265.73	−2.61	B1 III	7.11	+0.07	0.33	1140	···	+20	(275)	1,12
HD 74753	268.11	−4.49	B0 IVn	5.16	−0.22	0.08	700	470±120	+28	375	1,12
HD 74773	266.02	−2.76	B4 V	7.24	−0.12	0.06	480	840±410	+22	175	215
HD 74920	265.29	−1.95	O8	7.53	+0.03	0.34	1500	···	−9	251	5,16
HD 74979	261.11	+1.52	B0.5 IV	7.24	−0.05	0.00	1460	640±250	···	···	1,12
HD 75009	263.95	−0.75	B7.5 V	6.70	−0.09	0.02	230	350±70	(+16)	(200)	2,22
HD 75129	266.59	−2.74	B5 Ib:	6.87	+0.26	0.35	1980:	500±130	+10	···	2,23
HD 75149	265.33	−1.69	B3 Ia [v]	5.45	+0.27	0.40	1600	1010±550	+26	50	1,12
HD 75241	264.74	−1.09	B5 III	6.58	−0.13	0.03	550	310±60	+32	(90)	5,14
HD 75309	265.86	−1.90	B1 IIp	7.86	+0.01	0.25	2610	···	+35	(350)	112
HD 75387	262.83	+0.70	B2 IV-V [c]	6.42	−0.20	0.04	600	520±150	+30	(50)	1,12
HD 75534	267.01	−2.56	B1 Ib	7.82	+0.36	0.55	2650	···	+25	···	1,12
HD 75608	263.67	+0.30	B5.5 V	7.45	−0.09	0.06	420	340±76	···	···	2,22
HD 75759	262.80	+1.25	O9 V [s]	6.00	−0.11	0.20	860	590±180	+23	80	1,12
HD 75821	266.25	−1.54	B0 III [s]	5.11	−0.23	0.07	910	830±360	+7	60	1,13
HD 76004	264.56	+0.15	B3 V	6.35	−0.17	0.03	390	390±90	+22	150	7,18
HD 76161	267.89	−2.43	B3 Vn	5.90	−0.16	0.04	310	330±60	+13	(265)	3,13
HD 76534	264.42	+1.05	B2 Vpe [e]	8.02	+0.13	0.37	650	410±220	+17	260	2,15
HD 76566	265.64	+0.05	B3 IV	6.26	−0.16	0.04	530	290±50	+22	(40)	1,12
HD 76838	264.49	+1.46	B3 V [e]	7.31	+0.00	0.20	480	300±8	−18	···	2,12
HD 77320	264.82	+1.96	B2.5 Vne [e]	6.02	−0.14	0.09	290	310±50	···	(>300)	1,12
HD 78005	268.45	−0.38	B2.5 IV [v]	6.44	−0.15	0.08	550	350±70	+32	(50)	1,12
HD 79275	268.68	+1.14	B2 IV-V	5.79	−0.22	0.02	460	350±60	+7	(47)	1,12

[a]Information for stars observed. A ":" attached to an entry indicates an uncertain quantity.

[b]Additional information from the SIMBAD database is appended in square brackets. [c] = cluster member; [e] = emission line star; [m] = double or multiple star; [s] = spectroscopic or eclipsing binary; [v] = variable star

[c]Distance calculated from spectroscopic parallax and the standard reddening relation A_v =3.1 E(B-V).

[d]Distance and error calculated from Hipparcos parallax data.

[e]Listed radial velocities are heliocentric.

[f]B-V References: (1) Schild, Garrison, & Hiltner 1983; (2) Deutschman, Davis, & Schild 1976; (3) Johnson et al. 1966; (4) Loden 1968; (5) Cousins & Stoy 1962; (6) Hoffleit & Jaschek 1982; (7) Denoyelle 1977; (8) Moffat & Vogt 1975; (9) Cousins 1972; (10) Corbally 1984; (11) HD Catalogue

[g]MK References: (12) Garrison, Hiltner, & Schild 1977; (13) Hiltner, Garrison, & Schild 1969; (14) Feast, Thackeray, & Wesselink 1955; (15) Thackeray, Tritton, & Walker 1973; (16) Thackeray & Andrews 1974; (17) Feast et al. 1961; (18) Crampton 1971; (19) Buscombe 1969; (20) Roman 1978; (21) Morris 1961; (22) Tovmassian et al. 1993; (23) Houk 1978

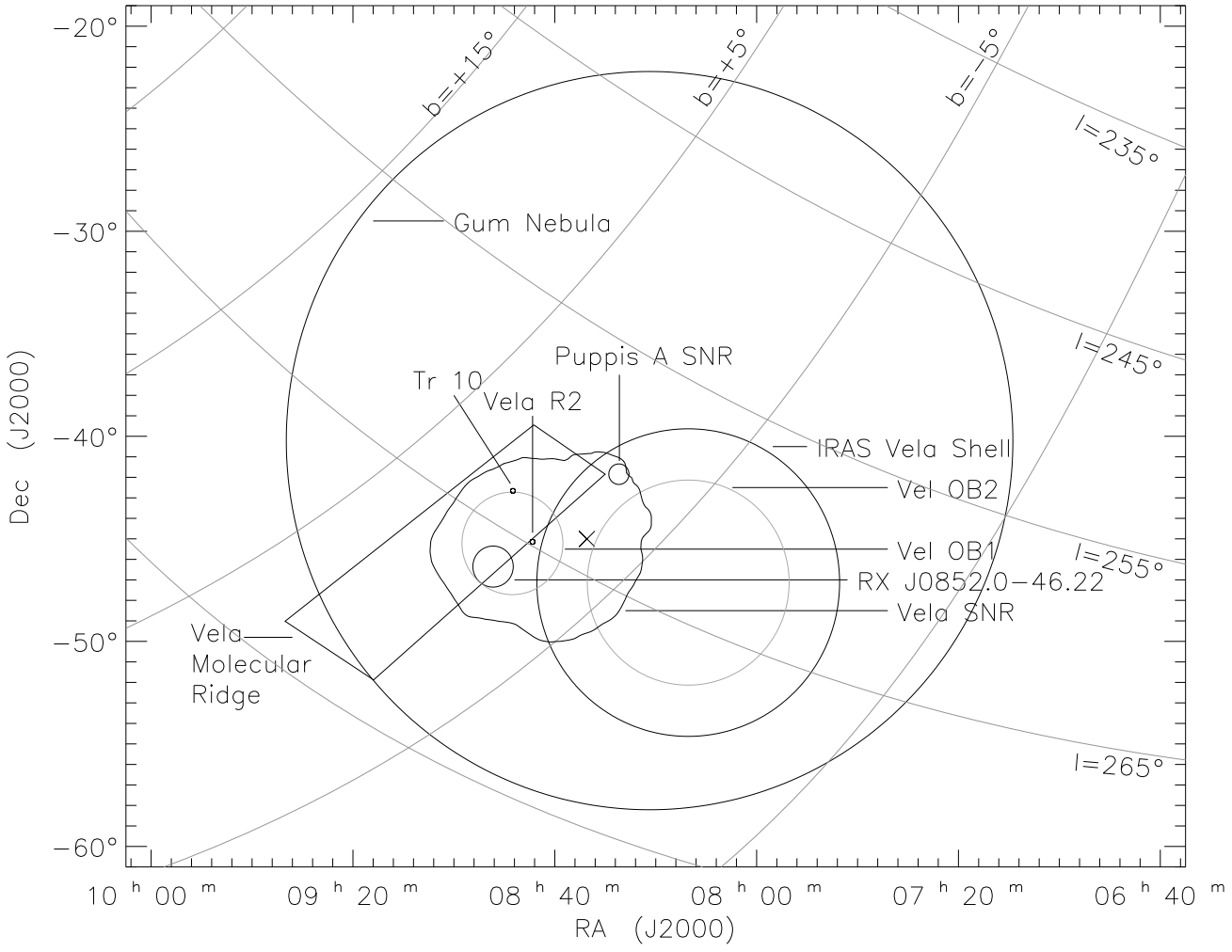
−20°
−30°
−40°
−50°
−60°
Dec (J2000)
10 h 00 m
09 h 20 m
08 h 40 m
08 h 00 m
07 h 20 m
06 h 40 m
RA (J2000)
b=+15°
b=+5°
b=−5°
l=235°
l=245°
l=255°
l=265°
Gum Nebula
Puppis A SNR
Tr 10
Vela R2
IRAS Vela Shell
Vel OB2
Vel OB1
RX J0852.0−46.22
Vela SNR
Vela
Molecular
Ridge

Figure 2

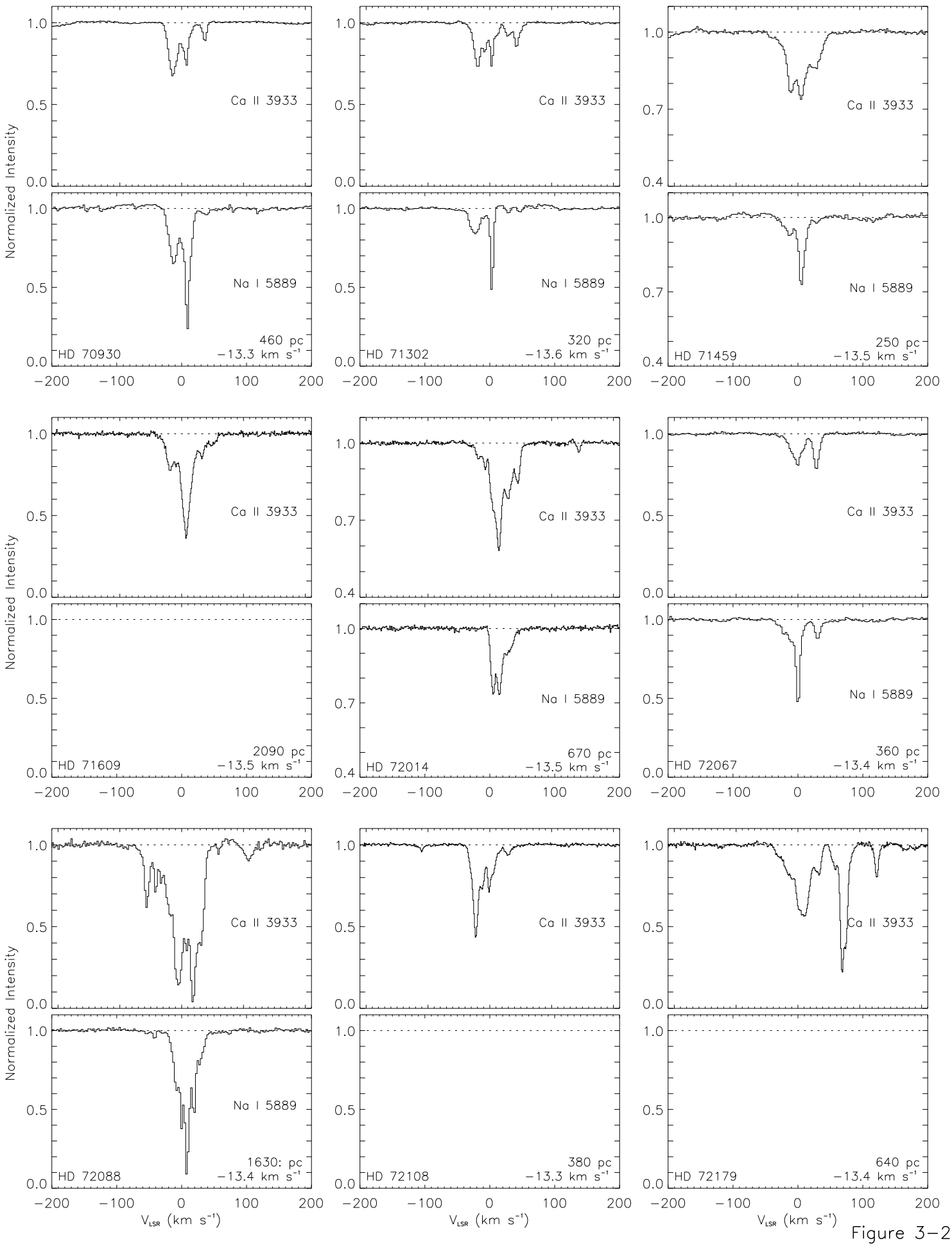
Normalized Intensity
Ca II 3933
Na I 5889
HD 70930
460 pc
−13.3 km s−1
HD 71302
320 pc
−13.6 km s−1
HD 71459
250 pc
−13.5 km s−1
HD 71609
2090 pc
−13.5 km s−1
HD 72014
670 pc
−13.5 km s−1
HD 72067
360 pc
−13.4 km s−1
HD 72088
1630: pc
−13.4 km s−1
HD 72108
380 pc
−13.3 km s−1
HD 72179
640 pc
−13.4 km s−1
VLSR (km s−1)

Figure 3–2

arXiv:astro-ph/9909128v1 7 Sep 1999

TABLE 2
Ca II Absorption Lines

Star	Obsv. Year	V_{LSR} ($km\,s^{-1}$)	W_λ(K) (mÅ)	Ref., Det.	Obsv. Year	V_{LSR} ($km\,s^{-1}$)	W_λ(K) (mÅ)	Obsv. Year	V_{LSR} ($km\,s^{-1}$)	W_λ(K) (mÅ)
HD 63308	···	···	···	···	1993	−15	29±1	···	···	···
	···	···	···	···	1993	+5	71±1	···	···	···
	···	···	···	···	1993	+16	123±1	···	···	···
	···	···	···	···	1993	+28	47±1	···	···	···
	···	···	···	···	1993	+45	5±1	···	···	···
HD 63578	1971-77	−14	68	1,p	1993	−14	24±1	···	···	···
	1971-77	+6	86	1,p	1993	+6	34±1	···	···	···
HD 65814	···	···	···	···	1993	−7	37±2	···	···	···
	···	···	···	···	1993	−1	30±3	···	···	···
	···	···	···	···	1993	+12	160±2	···	···	···
	···	···	···	···	1993	+23	27±1	···	···	···
	···	···	···	···	1993	+30	41±2	···	···	···
HD 68217	1971-77	−8	43	1,p	1994	−8	14±3	···	···	···
	1971-77	+5	22	1,p	1994	+9	20±2	···	···	···
HD 68243	···	···	···	···	1994	−12	8±1	···	···	···
	1971-77	+1	34	1,p	1994	0	24±2	···	···	···
	<1971	+1	51	4,p	···	···	···	···	···	···
HD 68324	···	···	···	···	1994	−5	25±1	···	···	···
	···	···	···	···	1994	+5	18±1	···	···	···
HD 69144	···	···	···	···	1994	−8	12±1	···	···	···
	···	···	···	···	1994	−1	8±3	···	···	···
	···	···	···	···	1994	+5	22±1	···	···	···
	···	···	···	···	1994	+17	5±1	···	···	···
HD 69302	···	···	···	···	···	···	···	1996	−23	5±1
	···	···	···	···	···	···	···	1996	−9	14±1
	···	···	···	···	···	···	···	1996	−1	8±1
	···	···	···	···	···	···	···	1996	+5	15±1
	···	···	···	···	···	···	···	1996	+6	60±1*
	···	···	···	···	···	···	···	1996	+40	6±1
HD 70309	···	···	···	···	···	···	···	1996	−28	14±1
	···	···	···	···	···	···	···	1996	−13	21±1
	1973	0	54	1,p	···	···	···	1996	+1	53±1
HD 70930	1973	−15	86	1,p	1993	−14	73±1	···	···	···
	1973	+4	86	1,p	···	···	···	···	···	···
	···	···	···	···	1993	+7	38±1	···	···	···
	···	···	···	···	1993	+37	12±1	···	···	···
HD 71302	···	···	···	···	1994	−20	49±1	···	···	···
	···	···	···	···	1994	−7	19±1	···	···	···
	···	···	···	···	1994	+3	19±1	···	···	···
	···	···	···	···	1994	+11	10±1	···	···	···
	···	···	···	···	1994	+29	11±1	···	···	···
	···	···	···	···	1994	+44	20±1	···	···	···
HD 71459	···	···	···	···	1993	−11	40±1	···	···	···
	···	···	···	···	1993	+5	53±1	···	···	···
	···	···	···	···	1993	+30	50±1	···	···	···

TABLE 2—*Continued*

Star	Obsv. Year	V_{LSR} ($km\,s^{-1}$)	W_λ(K) (mÅ)	Ref., Det.	Obsv. Year	V_{LSR} ($km\,s^{-1}$)	W_λ(K) (mÅ)	Obsv. Year	V_{LSR} ($km\,s^{-1}$)	W_λ(K) (mÅ)
HD 71609	···	···	···	···	···	···	···	1996	−20	35±1
	···	···	···	···	···	···	···	1996	−8	31±1
	···	···	···	···	···	···	···	1996	+6	107±1
	···	···	···	···	···	···	···	1996	+17	34±1
	···	···	···	···	···	···	···	1996	+32	22±1
	···	···	···	···	···	···	···	1996	+48	15±1
HD 72014	···	···	···	···	1993	−19	8±1	1996	−17	11±1
	···	···	···	···	1993	−8	7±1	1996	−7	6±1
	···	···	···	···	1993	+6	51±1	1996	+5	41±1
	···	···	···	···	1993	+15	38±3	1996	+15	45±1
	···	···	···	···	1993	+29	50±1	1996	+29	52±1
	···	···	···	···	1993	+45	17±1	1996	+46	16±1
HD 72067	1971-77	0	43	1,p	1994	−2	55±1	···	···	···
	1971-77	+30	54	1,p	1994	+30	32±1	···	···	···
HD 72088	···	···	···	···	1994	−56	50±1	···	···	···
	···	···	···	···	1994	−42	25±1	···	···	···
	···	···	···	···	1994	−33	23±1	···	···	···
	···	···	···	···	1994	−21	56±1	···	···	···
	···	···	···	···	1994	−5	206±1	···	···	···
	···	···	···	···	1994	+8	57±1	···	···	···
	···	···	···	···	1994	+18	129±1	···	···	···
	···	···	···	···	1994	+31	126±1	···	···	···
	···	···	···	···	1994	+108	20±1	···	···	···
HD 72089	<1983	−73	11	3,p	1993	−73	24±1	1996	−74	23±1
	···	···	···	···	1993	−40	9±1	1996	−40	10±1
	<1983	−9	21	3,p	1993	−8	45±1	1996	−10	53±1
	···	···	···	···	1993	+4	28±1	1996	+5	37±1
	<1983	+17	36	3,p	1993	+12	27±1	1996	+15	39±1
	1990	+23	197	2,d	1993	+20	40±1	1996	+22	21±1
	···	···	···	···	1993	+36	18±1	1996	+35	21±1
	···	···	···	···	1993	+45	8±1	1996	+45	9±1
	<1983	+76	92	3,p	1993	+74	124±1	1996	+74	126±1
	···	···	···	···	1993	+87	17±1	1996	+86	17±1
	···	···	···	···	1993	+92	22±1	1996	+93	30±1
	<1983	+108	37	3,p	1993	+105	90±1	1996	+106	75±1
	1990	+110	150	2,d	···	···	···	···	···	···
HD 72108	···	···	···	···	···	···	···	1996	−111	4±1
	1973	−36	85	1,p	···	···	···	···	···	···
	···	···	···	···	···	···	···	1996	−31	13±1
	···	···	···	···	···	···	···	1996	−23	67±1
	1973	−12	35	1,p	···	···	···	1996	−12	35±1
	···	···	···	···	···	···	···	1996	−1	20±1
	···	···	···	···	···	···	···	1996	+5	22±2
	···	···	···	···	···	···	···	1996	+29	11±1
HD 72127A	1981-88	−32	31	6,m	···	···	···	···	···	···
	1981-88	−28	63	6,m	1994	−28	71±1	1996	−28	92±1
	1971-77	−27	187	1,p	···	···	···	···	···	···

TABLE 2—*Continued*

Star	Obsv. Year	V_{LSR} ($km\,s^{-1}$)	W_λ(K) (mÅ)	Ref., Det.	Obsv. Year	V_{LSR} ($km\,s^{-1}$)	W_λ(K) (mÅ)	Obsv. Year	V_{LSR} ($km\,s^{-1}$)	W_λ(K) (mÅ)
	1981-88	−21	76	6,m	1994	−21	97±1	1996	−21	126±1
	1981-88	−7	113	6,m	1994	−10	76±1	1996	−10	68±1
	1971-77	−6	220	1,p	···	···	···	···	···	···
	1981-88	−1	66	6,m	1994	+1	105±1	1996	+1	111±1
	1981-88	+4	30	6,m	···	···	···	···	···	···
	1971-77	+13	102	1,p	···	···	···	···	···	···
	1981-88	+14	93	6,m	···	···	···	···	···	···
	1990	+17	582	2,d	1994	+17	104±1	1996	+16	103±1
	1971-77	+26	136	1,p	1994	+28	44±1	1996	+27	47±1
	1981-88	+27	64	6,m	···	···	···	···	···	···
	1971-77	+41	86	1,p	···	···	···	···	···	···
	1981-88	+42	56	6,m	1994	+42	48±1	1996	+42	52±1
	1981-88	+48	43	6,m	···	···	···	···	···	···
HD 72127B	···	···	···	···	···	···	···	1996	−28	61±1
	···	···	···	···	···	···	···	1996	−19	45±1
	···	···	···	···	···	···	···	1996	−10	35±1
	···	···	···	···	···	···	···	1996	0	243±1
	1990	+1	609	2,d	···	···	···	1996	+17	81±1
	···	···	···	···	···	···	···	1996	+27	31±1
	···	···	···	···	···	···	···	1996	+42	64±1
HD 72179	···	···	···	···	···	···	···	1996	−33	6±1
	···	···	···	···	···	···	···	1996	−12	66±1
	···	···	···	···	···	···	···	1996	+1	11±2
	···	···	···	···	···	···	···	1996	+11	117±2
	···	···	···	···	···	···	···	1996	+29	10±1
	···	···	···	···	···	···	···	1996	+35	17±3
	···	···	···	···	···	···	···	1996	+61	26±1
	···	···	···	···	···	···	···	1996	+71	65±3
	···	···	···	···	···	···	···	1996	+78	50±3
	···	···	···	···	···	···	···	1996	+84	15±2
	···	···	···	···	···	···	···	1996	+127	19±1
HD 72232	1971-77	···	<34	1,p	1994	+2	15±1	···	···	···
	···	···	···	···	1994	+3	117±2⋆	···	···	···
	···	···	···	···	1994	+10	6±1	···	···	···
HD 72350	···	···	···	···	1994	−6	28±1	···	···	···
	···	···	···	···	1994	0	25±1	···	···	···
	<1983	+6	113	3,p	1994	+7	67±1	···	···	···
	1971-77	+7	···	1,p	···	···	···	···	···	···
	1971-77	+18	311	1,p	···	···	···	···	···	···
	<1983	+21	136	3,p	1994	+20	133±1	···	···	···
	1990	+26	335	2,d	···	···	···	···	···	···
	<1983	+40	37	3,p	1994	+38	48±1	···	···	···
	···	···	···	···	1994	+114	4±1	···	···	···
	···	···	···	···	1994	+122	3±1	···	···	···
HD 72485	···	···	···	···	1994	−17	11±2	···	···	···
	···	···	···	···	1994	-2	147±2⋆	···	···	···
	···	···	···	···	1994	+7	16±1	···	···	···

TABLE 2—*Continued*

Star	Obsv. Year	V_{LSR} ($km\,s^{-1}$)	W_λ(K) (mÅ)	Ref., Det.	Obsv. Year	V_{LSR} ($km\,s^{-1}$)	W_λ(K) (mÅ)	Obsv. Year	V_{LSR} ($km\,s^{-1}$)	W_λ(K) (mÅ)
	···	···	···	···	1994	+27	17±1	···	···	···
HD 72535	···	···	···	···	···	···	···	1996	−9	8±1
	···	···	···	···	···	···	···	1996	+10	142±1
	···	···	···	···	···	···	···	1996	+21	44±1
	···	···	···	···	···	···	···	1996	+29	42±1
HD 72555	1973	−15	···	1,p	1994	−16	56±1	···	···	···
	···	···	···	···	1994	−8	14±1	···	···	···
	1973	+1	108	1,p	1994	0	41±1	···	···	···
	···	···	···	···	1994	+10	37±1	···	···	···
	···	···	···	···	1994	+27	11±1	···	···	···
HD 72648	···	···	···	···	1993	−9	24±1	···	···	···
	···	···	···	···	1993	+10	103±2	···	···	···
	1990	+35	623	2,d	1993	+36	321±1	···	···	···
	···	···	···	···	1993	+57	11±3	···	···	···
HD 72798	···	···	···	···	1994	−25	19±1	···	···	···
	···	···	···	···	1994	−10	40±1	···	···	···
	···	···	···	···	1994	+2	82±3	···	···	···
	1971-77	+15	274	1,p	1994	+18	96±2	···	···	···
	···	···	···	···	1994	+29	13±2	···	···	···
	···	···	···	···	1994	+39	20±2	···	···	···
HD 72800	···	···	···	···	···	···	···	1996	−35	26±1
	···	···	···	···	···	···	···	1996	−10	106±1
	···	···	···	···	···	···	···	1996	+7	124±1
	···	···	···	···	···	···	···	1996	+21	90±2
	···	···	···	···	···	···	···	1996	+21	470±2*
HD 72997	···	···	···	···	1993	−20	37±1	1996	−18	32±1
	···	···	···	···	1993	−3	52±1	1996	−5	42±1
	···	···	···	···	1993	+9	35±1	1996	+7	46±1
	···	···	···	···	1993	+20	12±1	1996	+19	20±1
	···	···	···	···	1993	+32	63±1	1996	+31	63±1
	···	···	···	···	1993	+190	23±1	1996	+191	19±1
HD 73326	···	···	···	···	···	···	···	1996	−46	14±1
	···	···	···	···	···	···	···	1996	−37	18±1
	···	···	···	···	···	···	···	1996	−10	50±1
	···	···	···	···	···	···	···	1996	0	7±2
	···	···	···	···	···	···	···	1996	+7	48±1
	···	···	···	···	···	···	···	1996	+17	36±1
HD 73478	···	···	···	···	···	···	···	1996	−36	10±1
	···	···	···	···	···	···	···	1996	−22	44±1
	···	···	···	···	···	···	···	1996	−8	73±1
	···	···	···	···	···	···	···	1996	+5	70±1
	···	···	···	···	···	···	···	1996	+13	51±2
HD 73658	···	···	···	···	1993	-126	5±1	1996	-126	4±1
	···	···	···	···	1993	−33	41±1	1996	−32	4±2
	···	···	···	···	1993	−15	144±1	1996	−15	91±1
	···	···	···	···	1993	−2	51±1	1996	-3	42±1
	···	···	···	···	1993	+7	126±1	1996	+6	140±1

TABLE 2—*Continued*

Star	Obsv. Year	V_{LSR} ($km\,s^{-1}$)	W_λ(K) (mÅ)	Ref., Det.	Obsv. Year	V_{LSR} ($km\,s^{-1}$)	W_λ(K) (mÅ)	Obsv. Year	V_{LSR} ($km\,s^{-1}$)	W_λ(K) (mÅ)
	···	···	···	···	1993	+18	68±1	1996	+17	36±2
	1990	+21	507	2,d	···	···	···	···	···	···
	···	···	···	···	1993	+25	58±1	1996	+24	67±1
HD 74194	···	···	···	···	1993	−141	30±1	1996	−140	23±1
	···	···	···	···	1993	−88	11±1	1996	−89	9±1
	···	···	···	···	1993	−78	14±1	1996	−79	12±1
	1973	−63	172	1,p	1993	−61	31±1	1996	−61	20±1
	···	···	···	···	1993	−49	10±1	1996	−55	31±1
	···	···	···	···	1993	−17	50±1	1996	−20	50±1
	···	···	···	···	1993	−7	21±1	1996	−8	26±1
	1973	+8	252	1,p	1993	+9	133±1	1996	+8	134±1
HD 74234	···	···	···	···	···	···	···	1996	−17	27±1
	<1983	−3	20	3,p	···	···	···	1996	−6	18±1
	1973	+2	216	1,p	···	···	···	···	···	···
	<1983	+6	180	3,p	···	···	···	1996	+5	64±1
	···	···	···	···	···	···	···	1996	+28	15±1
	···	···	···	···	···	···	···	1996	+69	47±1
	···	···	···	···	···	···	···	1996	+85	6±1
HD 74251	···	···	···	···	···	···	···	1996	−108	8±1
	···	···	···	···	···	···	···	1996	−5	41±1
	···	···	···	···	···	···	···	1996	+6	56±1
	1973	+8	216	1,p	···	···	···	···	···	···
	···	···	···	···	···	···	···	1996	+16	40±1
	···	···	···	···	···	···	···	1996	+78	5±1
	···	···	···	···	···	···	···	1996	+86	9±1
HD 74273	···	···	···	···	1994	−25	21±1	1996	−27	11±1
	···	···	···	···	1994	−9	51±1	1996	−9	66±1
	<1971	−1	117	4,p	···	···	···	···	···	···
	1971	+2	172	1,p	···	···	···	···	···	···
	···	···	···	···	1994	+5	43±1	1996	+6	34±1
HD 74319	···	···	···	···	1994	−19	15±1	···	···	···
	···	···	···	···	1994	−7	29±1	···	···	···
	···	···	···	···	1994	+8	41±1	···	···	···
	···	···	···	···	1994	+19	38±1	···	···	···
HD 74371	···	···	···	···	1994	−10	42±2	···	···	···
	<1971	−5	304	4,p	···	···	···	···	···	···
	1971	−2	···	1,p	1994	+2	286±3•	···	···	···
	<1971	+10	330	4,p	1994	+11	96±2	···	···	···
	1971	+13	···	1,p ···	···	···	···	···	···	
	···	···	···	···	1994	+29	301±3•	···	···	···
HD 74436	···	···	···	···	1994	−7	57±1	···	···	···
	···	···	···	···	1994	+7	80±1	···	···	···
HD 74455	···	···	···	···	1994	−183	6±1	1996	−182	5±1
	<1971	−174	36	4,p	1994	−173	39±1	1996	−173	21±1
	1971-73	−173	43	1,p	···	···	···	···	···	···
	<1971	−166	···	5,p	1994	−166	6±1	1996	−166	8±1
	1990	−159	28	2,d	···	···	···	···	···	···

TABLE 2—*Continued*

Star	Obsv. Year	V_{LSR} ($km\,s^{-1}$)	W_λ(K) (mÅ)	Ref., Det.	Obsv. Year	V_{LSR} ($km\,s^{-1}$)	W_λ(K) (mÅ)	Obsv. Year	V_{LSR} ($km\,s^{-1}$)	W_λ(K) (mÅ)
	<1971	−70	···	5,p	···	···	···	···	···	···
	<1971	−24	···	5,p	···	···	···	···	···	···
	1971-73	−6	68	1,p	1994	−13	56±1	1996	−14	55±1
	···	···	···	···	1994	−4	14±1	1996	−2	34±1
	<1971	+5	204	4,p	1994	+6	99±1	1996	+7	88±1
	<1971	+5	···	5,p	···	···	···	···	···	···
	1971-73	+7	108	1,p	···	···	···	···	···	···
	1990	+18	216	2,d	···	···	···	···	···	···
HD 74530	···	···	···	···	1994	−69	30±1	···	···	···
	···	···	···	···	1994	−5	67±1	···	···	···
	···	···	···	···	1994	+7	61±1	···	···	···
	···	···	···	···	1994	+13	41±1	···	···	···
HD 74531	1973	−152	34	1,p	···	···	···	···	···	···
	···	···	···	···	1994	−141	34±1	1996	−141	25±1
	1973	+5	216	1,p	1994	+7	70±1	1996	+7	94±1
HD 74650	···	···	···	···	···	···	···	1996	−1	8±1
	···	···	···	···	···	···	···	1996	+6	21±1
HD 74662	···	···	···	···	···	···	···	1996	−19	6±2
	···	···	···	···	···	···	···	1996	−10	54±2
	···	···	···	···	···	···	···	1996	−2	14±4
	···	···	···	···	···	···	···	1996	+2	152±3•
	···	···	···	···	···	···	···	1996	+6	47±3
HD 74711	···	···	···	···	1993	−4	55±2	···	···	···
	···	···	···	···	1993	+5	59±2	···	···	···
	···	···	···	···	1993	+14	55±2	···	···	···
	···	···	···	···	1993	+27	46±1	···	···	···
HD 74753	1971	−8	172	1,p	1994	−9	53±1	···	···	···
	<1971	−8	122	4,p	···	···	···	···	···	···
	···	···	···	···	1994	+2	39±1	···	···	···
HD 74773	···	···	···	···	1994	−18	48±1	1996	−17	59±1
	···	···	···	···	1994	−11	43±1	1996	−9	26±1
	···	···	···	···	1994	+5	49±2	1996	+5	50±1
	···	···	···	···	1994	+18	26±2	1996	+18	25±1
	···	···	···	···	1994	+27	46±1	1996	+27	44±1
HD 74920	···	···	···	···	1993	−36	23±2	···	···	···
	···	···	···	···	1993	−23	50±2	···	···	···
	<1971	−8	122	4,p	1993	−9	34±3	···	···	···
	···	···	···	···	1993	−3	42±1	···	···	···
	<1983	+6	40	3,p	1993	+2	35±4	···	···	···
	···	···	···	···	1993	+10	134±2	···	···	···
	···	···	···	···	1993	+21	40±3	···	···	···
	···	···	···	···	1993	+45	14±1	···	···	···
HD 74979	···	···	···	···	···	···	···	1996	−87	15±1
	···	···	···	···	···	···	···	1996	−13	9±1
	···	···	···	···	···	···	···	1996	+1	73±1
	···	···	···	···	···	···	···	1996	+12	146±1
HD 75009	···	···	···	···	1994	−22	10±1	···	···	···

TABLE 2—*Continued*

Star	Obsv. Year	V_{LSR} ($km\,s^{-1}$)	W_λ(K) (mÅ)	Ref., Det.	Obsv. Year	V_{LSR} ($km\,s^{-1}$)	W_λ(K) (mÅ)	Obsv. Year	V_{LSR} ($km\,s^{-1}$)	W_λ(K) (mÅ)
	···	···	···	···	1994	−8	7±1	···	···	···
	···	···	···	···	1994	+6	19±1	···	···	···
HD 75129	···	···	···	···	···	···	···	1996	−98	26±1
	···	···	···	···	···	···	···	1996	−67	62±1
	···	···	···	···	···	···	···	1996	+2	396±2•
	···	···	···	···	···	···	···	1996	+7	109±1
HD 75149	···	···	···	···	1994	−24	59±2•	···	···	···
	···	···	···	···	1994	−19	14±1	···	···	···
	···	···	···	···	1994	−9	43±1	···	···	···
	···	···	···	···	1994	+8	163±1	···	···	···
	<1971	+8	450	4,p	···	···	···	···	···	···
	···	···	···	···	1994	+13	213±1⋆	···	···	···
	···	···	···	···	1994	+28	52±1	···	···	···
HD 75241	···	···	···	···	1994	−52	11±1	···	···	···
	···	···	···	···	1994	−40	12±1	···	···	···
	···	···	···	···	1994	−27	31±1	···	···	···
	···	···	···	···	1994	−22	41±1	···	···	···
	···	···	···	···	1994	−9	45±1	···	···	···
	···	···	···	···	1994	+6	30±1	···	···	···
	···	···	···	···	1994	+17	6±1	···	···	···
	···	···	···	···	1994	+28	44±1	···	···	···
	···	···	···	···	1994	+37	8±1	···	···	···
	···	···	···	···	1994	+47	9±1	···	···	···
HD 75309	···	···	···	···	1993	−118	12±1	1996	−120	16±1
	···	···	···	···	1993	−74	12±2	1996	−72	20±1
	···	···	···	···	1993	−6	130±1	1996	−5	158±1
	···	···	···	···	1993	+7	53±2	1996	+7	71±1
	···	···	···	···	1993	+14	146±2	1996	+17	60±1
	···	···	···	···	1993	+38	7±2	1996	+38	16±1
	···	···	···	···	1993	+54	47±1	1996	+53	39±1
	···	···	···	···	1993	+81	4±2	1996	+81	<1
	···	···	···	···	1993	+89	7±2	1996	+89	<1
	···	···	···	···	1993	+123	9±1	1996	+123	7±1
HD 75387	···	···	···	···	1994	−39	14±1	···	···	···
	···	···	···	···	1994	−20	25±1	···	···	···
	···	···	···	···	1994	−9	14±1	···	···	···
	···	···	···	···	1994	+3	60±1	···	···	···
	···	···	···	···	1994	+17	44±1⋆	···	···	···
HD 75534	···	···	···	···	···	···	···	1996	−46	8±1
	···	···	···	···	···	···	···	1996	−17	32±1
	···	···	···	···	···	···	···	1996	−5	62±1
	···	···	···	···	···	···	···	1996	+5	128±1
	···	···	···	···	···	···	···	1996	+13	72±1
	···	···	···	···	···	···	···	1996	+23	62±1
HD 75608	···	···	···	···	···	···	···	1996	−37	8±1
	···	···	···	···	···	···	···	1996	−27	21±2
	···	···	···	···	···	···	···	1996	−19	14±2

TABLE 2—*Continued*

Star	Obsv. Year	V_{LSR} ($km\,s^{-1}$)	W_λ(K) (mÅ)	Ref., Det.	Obsv. Year	V_{LSR} ($km\,s^{-1}$)	W_λ(K) (mÅ)	Obsv. Year	V_{LSR} ($km\,s^{-1}$)	W_λ(K) (mÅ)
	···	···	···	···	···	···	···	1996	−9	12±1
	···	···	···	···	···	···	···	1996	+4	26±1
	···	···	···	···	···	···	···	1996	+25	12±1
HD 75759	···	···	···	···	1994	−40	11±1	···	···	···
	···	···	···	···	1994	−19	12±1	···	···	···
	1971-77	+7	108	1,p	1994	+5	45±1	···	···	···
	···	···	···	···	1994	+15	32±1	···	···	···
HD 75821	<1971	−126	39	5,p	···	···	···	···	···	···
	···	···	···	···	1993	−98	21±1	1996	−99	26±1
	<1971	−88	73	4,p	···	···	···	···	···	···
	<1971	−89	59	5,p	···	···	···	···	···	···
	1971	−86	108	1,p	1993	−85	66±1	1996	−85	53±1
	1971	−9	54	1,p	1993	−9	30±1	1996	−10	30±1
	<1971	+3	140	5,p	1993	+1	23±1	1996	0	22±1
	<1971	+4	95	4,p	···	···	···	···	···	···
	1971	+9	108	1,p	1993	+10	41±1	1996	+9	39±1
	1990	+21	157	2,d	···	···	···	···	···	···
	1971	+24	17	1,p	1993	+23	28±1	1996	+22	26±1
HD 76004	···	···	···	···	1994	−20	31±2	···	···	···
	···	···	···	···	1994	−6	19±5	···	···	···
	···	···	···	···	1994	+5	24±4	···	···	···
	···	···	···	···	1994	+10	11±7	···	···	···
	···	···	···	···	1994	+24	11±2	···	···	···
	···	···	···	···	1994	+33	34±2	···	···	···
HD 76161	···	···	···	···	1993	−8	16±1	···	···	···
	1971	−1	34	1,p	···	···	···	···	···	···
	<1971	0	51	4,p	1993	+2	38±2	···	···	···
HD 76534	···	···	···	···	1994	−86	7±2	···	···	···
	···	···	···	···	1994	−27	16±1	···	···	···
	···	···	···	···	1994	−17	18±1	···	···	···
	···	···	···	···	1994	−4	13±2	···	···	···
	···	···	···	···	1994	+8	64±2	···	···	···
	···	···	···	···	1994	+16	28±3	···	···	···
	···	···	···	···	1994	+32	13±1	···	···	···
HD 76566	1973	−18	172	1,p	1994	−20	31±1	···	···	···
	···	···	···	···	1994	−10	15±1	···	···	···
	···	···	···	···	1994	+6	68±1	···	···	···
	···	···	···	···	1994	+15	53±2	···	···	···
HD 76838	···	···	···	···	···	···	···	1996	−18	24±1
	···	···	···	···	···	···	···	1996	+9	65±1
	···	···	···	···	···	···	···	1996	+17	7±1
	···	···	···	···	···	···	···	1996	+33	7±1
HD 77320	···	···	···	···	1994	−20	18±1	···	···	···
	···	···	···	···	1994	−8	3±1	···	···	···
	1971-77	−4	34	1,p	···	···	···	···	···	···
	···	···	···	···	1994	+3	16±1	···	···	···
	···	···	···	···	1994	+36	4±1	···	···	···

TABLE 2—*Continued*

Star	Obsv. Year	V_{LSR} ($km\,s^{-1}$)	W_λ(K) (mÅ)	Ref., Det.	Obsv. Year	V_{LSR} ($km\,s^{-1}$)	W_λ(K) (mÅ)	Obsv. Year	V_{LSR} ($km\,s^{-1}$)	W_λ(K) (mÅ)
HD 78005	···	···	···	···	1994	−24	9±1	···	···	···
	···	···	···	···	1994	+3	135±3	···	···	···
	···	···	···	···	1994	+19	26±2⋆	···	···	···
	···	···	···	···	1994	+33	35±2	···	···	···
HD 79275	···	···	···	···	1994	−28	30±1	···	···	···
	···	···	···	···	1994	−13	78±1	···	···	···
	···	···	···	···	1994	+1	91±1	···	···	···

⋆Broad absorption feature with central velocity corresponding to the star's radial velocity.

•Broad absorption feature, possibly interstellar in origin.

Ref. 1: Wallerstein, Silk, & Jenkins 1980, CTIO 1.5m coudé spectrograph with dispersion = 4.5 or 9 Å mm^{-1} and 9 or 18 Å mm^{-1} for Ca II and Na I, respectively.

Ref 2: Wallerstein & Gilroy, 1992, CTIO 4m echelle spectrograph with R = 20,000.

Ref 3: Jenkins, Wallerstein, & Silk, 1984, CTIO 4m echelle spectrograph with dispersion = 2.2 Å mm^{-1} and 3.3 Å mm^{-1} for Ca II and Na I, respectively.

Ref. 4: Wallerstein & Silk, 1971, CTIO 60-inch telescope and coudé spectrograph with R_{CaII}= 20,000 & R_{NaI}= 15,000.

Ref. 5: Thackeray & Warren, 1972, Radcliffe coudé spectrograph with dispersion = 6.8 Å mm^{-1}.

Ref. 6: Hobbs et al., 1991, McDonald 2.7m coudé spectrograph and ESO CAT 1.4m with $R_{1981-1984}$= 55,000 & $R_{1986-1988}$= 110,000. Velocities and equivalent widths cited are an average of nine data sets obtained between 1981 and 1988.

Detectors used for observations: d–CCD; p–photographic plate; m–multiple observations using two or more of the following detectors: photo-multiplier tube, digicon, reticon, CCD.

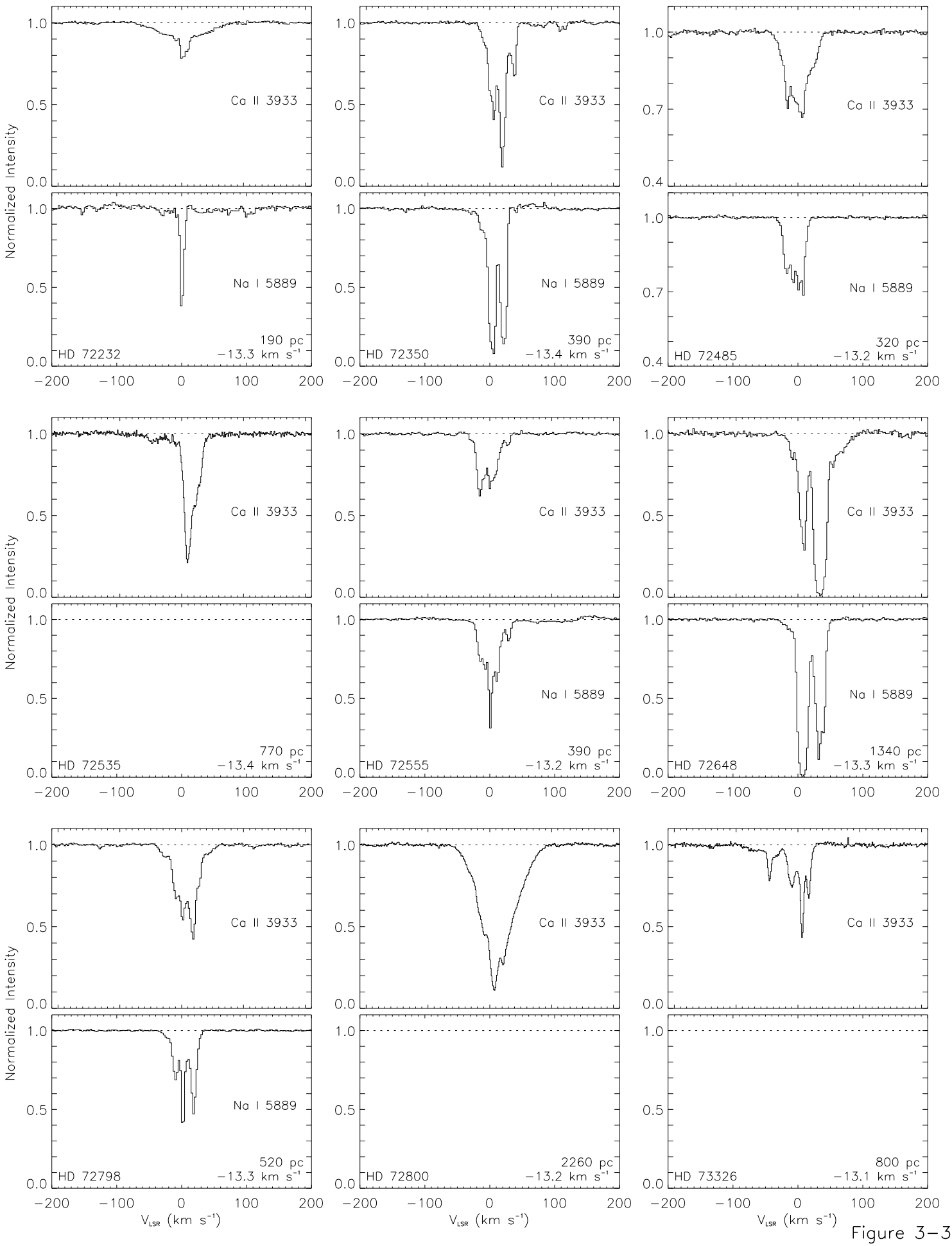
Normalized Intensity
Ca II 3933
Na I 5889
HD 72232
190 pc
−13.3 km s−1
HD 72350
390 pc
−13.4 km s−1
HD 72485
320 pc
−13.2 km s−1
HD 72535
770 pc
−13.4 km s−1
HD 72555
390 pc
−13.2 km s−1
HD 72648
1340 pc
−13.3 km s−1
HD 72798
520 pc
−13.3 km s−1
HD 72800
2260 pc
−13.2 km s−1
HD 73326
800 pc
−13.1 km s−1
VLSR (km s−1)

Figure 3–3

arXiv:astro-ph/9909128v1 7 Sep 1999

TABLE 3

Na I Absorption Lines

Star	Obsv. Year	V_{LSR} ($km\,s^{-1}$)	$W_\lambda(D_2,D_1)$ (mÅ)	Ref.,[a] Det.	Obsv. Year	V_{LSR}[b] ($km\,s^{-1}$)	$W_\lambda(D_2,D_1)$ (mÅ)	Obsv. Year	V_{LSR}[b] ($km\,s^{-1}$)	$W_\lambda(D_2,D_1)$ (mÅ)
HD 63578	···	···	···	···	1993	−4	223,178±1	···	···	···
	1971-77	+8	246,123	1,p	1993	+11	325,270±1	···	···	···
HD 65814	···	···	···	···	1993	+1	267,138±1	···	···	···
	···	···	···	···	1993	+14	354,304±1	···	···	···
	···	···	···	···	1993	+31	128,104±1	···	···	···
HD 68217	···	···	···	···	1994	−18	17±1,<6	···	···	···
	···	···	···	···	1994	−8	30,20±3	···	···	···
	···	···	···	···	1994	+2	43,12±1	···	···	···
	···	···	···	···	1994	+9	20,16±2	···	···	···
HD 68243	···	···	···	···	1994	−8	23,10±1	···	···	···
	···	···	···	···	1994	−2	33,25±2	···	···	···
HD 68324	···	···	···	···	1994	−1	124,63±1	···	···	···
HD 69144	···	···	···	···	1994	−8	60,20±1	···	···	···
	···	···	···	···	1994	0	66,44±2	···	···	···
	···	···	···	···	1994	+9	24,13±1	···	···	···
HD 70930	···	···	···	···	1993	−10	131,66±1	···	···	···
	1971-77	+5	490,246	1,p	···	···	···	···	···	···
	···	···	···	···	1993	+9	138,84±1	···	···	···
HD 71302	···	···	···	···	1994	−23	61,24±1	···	···	···
	···	···	···	···	1994	+3	58,46±3	···	···	···
HD 71459	···	···	···	···	1993	−14	24±1,<6	···	···	···
	···	···	···	···	1993	+6	60,32±1	···	···	···
HD 72014	···	···	···	···	1993	+5	55,21±1	1996	+5	43,23±1
	···	···	···	···	1993	+15	43,19±2	1996	+15	38,19±1
	···	···	···	···	1993	+28	54,33±1	1996	+27	42,20±1
HD 72067	···	···	···	···	1994	−23	17±1,<6	···	···	···
	···	···	···	···	1994	−10	27,16±1	···	···	···
	···	···	···	···	1994	+1	100,46±2	···	···	···
	···	···	···	···	1994	+31	23,13±1	···	···	···
HD 72088	···	···	···	···	1994	−42	6±1,<6	···	···	···
	···	···	···	···	1994	−8	91,39±1	···	···	···
	···	···	···	···	1994	+1	60,41±4	···	···	···
	···	···	···	···	1994	+8	147,114±2	···	···	···
	···	···	···	···	1994	+18	77,52±1	···	···	···
	···	···	···	···	1994	+29	52,23±1	···	···	···
HD 72089	<1983	−12	138,74	3,p	1993	−10	127,76±1	1996	−10	118,70±1
	<1983	+2	93,47[c]	3,p	1993	+2	89,47±1	1996	+2	68,42±1
	<1983	+17	74,36	3,p	1993	+12	51,34±1	1996	+11	52,33±1
	···	···	···	···	1993	+21	77,43±2	1996	+20	77,46±1
	···	···	···	···	1993	+76	12,6±1	1996	+75	14±1,<6
	···	···	···	···	1993	+104	56,30±2	1996	+106	23,9±1
HD 72127A	1981-88	−28	16,8	6,m	1994	−28	13±1,<6	···	···	···
	1981-88	−21	8,4	6,m	···	···	···	···	···	···
	1981-88	−13	23,12	6,m	1994	−19	18±3,<6	···	···	···
	1981-88	−6	66,33	6,m	1994	−9	46,26±2	···	···	···

TABLE 3—*Continued*

Star	Obsv. Year	V_{LSR} ($km\,s^{-1}$)	$W_\lambda(D_2,D_1)$ (mÅ)	Ref.,[a] Det.	Obsv. Year	V_{LSR}[b] ($km\,s^{-1}$)	$W_\lambda(D_2,D_1)$ (mÅ)	Obsv. Year	V_{LSR}[b] ($km\,s^{-1}$)	$W_\lambda(D_2,D_1)$ (mÅ)
	1971-77	−1	50,25	1,p	···	···	···	···	···	···
	1981-88	−1	120,61	6,m	1994	+1	102,82±1	···	···	···
	1981-88	+4	50,25	6,m	···	···	···	···	···	···
	1981-88	+21	25,13	6,m	1994	+22	6±1,<6	···	···	···
	1981-88	+41	8,4	6,m	···	···	···	···	···	···
HD 72232	···	···	···	···	1994	−29	11±1,<6	···	···	···
	···	···	···	···	1994	+1	84,58±1	···	···	···
	1971-77	+5	246,123	1,p	···	···	··· ···	···	···	
HD 72350	···	···	···	···	1994	−12	36,15±1	···	···	···
	<1983	+2	275,224	3,p	1994	+4	259,227±1	···	···	···
	1971-77	+12	452,449	1,p	···	···	···	···	···	···
	<1983	+18	251,224	3,p	1994	+21	206,206±1	···	···	···
HD 72485	···	···	···	···	1994	−17	61,22±1	···	···	···
	···	···	···	···	1994	−7	31,20±2	···	···	···
	···	···	···	···	1994	0	42,16±8	···	···	···
	···	···	···	···	1994	+8	50,25±2	···	···	···
HD 72555	···	···	···	···	1994	−14	58,26±1	···	···	···
	···	···	···	···	1994	−7	30,16±2	···	···	···
	1971-77	+3	314,204	1,p	1994	+1	80,60±2	···	···	···
	···	···	···	···	1994	+10	97,51±1	···	···	···
	···	···	···	···	1994	+29	26,12±1	···	···	···
HD 72648	···	···	···	···	1993	+8	387,326±1	···	···	···
	···	···	···	···	1993	+32	222,148±1	···	···	···
	···	···	···	···	1993	+41	76,50±2	···	···	···
HD 72798	···	···	···	···	1994	−10	69,31±1	···	···	···
	···	···	···	···	1994	+2	86,52±1	···	···	···
	···	···	···	···	1994	+18	117,65±1	···	···	···
HD 72997	···	···	···	···	1993	0	67,38±1	1996	0	67,31±1
	···	···	···	···	1993	+27	67,35±1	1996	+27	70,36±1
	···	···	···	···	1993	+190	16±1,<6	1996	+191	15,7±1
HD 73658	···	···	···	···	1993	−10	82,46±1	1996	−11	76,46±1
	···	···	···	···	1993	+7	269,231±1	1996	+7	264,218±1
	···	···	···	···	1993	+20	81,40±1	1996	+19	80,47±1
HD 74194	1971-77	···	<62,<31	1,p	1993	−19	27,14±1	1996	−24	15,10±1
	···	···	···	···	1993	−7	44,26±1	1996	−8	58,23±1
	1971-77	+10	522,390	1,p	1993	+9	355,308±2	1996	+9	348,310±1
	···	···	···	···	1993	+23	71,50±1	1996	+23	55,37±1
HD 74273	···	···	···	···	1994	−27	10±1,<6	1996	−27	8,6±1
	···	···	···	···	1994	−11	73,30±1	1996	−12	68,26±1
	···	···	···	···	1994	+5	124,70±1	1996	+5	121,75±1
	···	···	···	···	1994	+20	15,18±10	1996	+19	39,17±1
HD 74319	···	···	···	···	1994	−29	14±1,<6	···	···	···
	···	···	···	···	1994	−7	84,38±5	···	···	···
	···	···	···	···	1994	+9	81,55±1	···	···	···
	···	···	···	···	1994	+20	104,88±1	···	···	···
HD 74455	···	···	···	···	1994	−11	64,26±1	1996	−12	59,37±1
	···	···	···	···	1994	0	40,23±2	1996	0	27,34±1

TABLE 3—*Continued*

Star	Obsv. Year	V_{LSR} ($km\,s^{-1}$)	$W_\lambda(D_2,D_1)$ (mÅ)	Ref.,[a] Det.	Obsv. Year	V_{LSR}[b] ($km\,s^{-1}$)	$W_\lambda(D_2,D_1)$ (mÅ)	Obsv. Year	V_{LSR}[b] ($km\,s^{-1}$)	$W_\lambda(D_2,D_1)$ (mÅ)
	<1971	+8	426,234	4,p	···	···	···	···	···	···
	1971-77	+12	438,295	1,p	1994	+11	246,180±2	1996	+10	264,190±1
	<1971	···	<50,<50	4,p	···	···	···	···	···	···
HD 74530	···	···	···	···	1994	−12	49,26±1	···	···	···
	···	···	···	···	1994	0	64,25±1	···	···	···
	···	···	···	···	1994	+11	226,199±1	···	···	···
HD 74531	···	···	···	···	1994	−13	51,28±1	···	···	···
	···	···	···	···	1994	+2	88,35±2	···	···	···
	···	···	···	···	1994	+8	126,114±2	···	···	···
	···	···	···	···	1994	+14	89,63±2	···	···	···
HD 74711	···	···	···	···	1993	−10	42,20±1	···	···	···
	···	···	···	···	1993	+9	426,366±1	···	···	···
	···	···	···	···	1993	+28	49,27±1	···	···	···
HD 74753	···	···	···	···	1994	−21	18±1,<6	···	···	···
	···	···	···	···	1994	−8	53,25±2	···	···	···
	···	···	···	···	1994	+1	46,34±3	···	···	···
	···	···	···	···	1994	+7	94,51±2	···	···	···
	···	···	···	···	1994	+16	31,28±1	···	···	···
HD 74773	···	···	···	···	1994	−17	43,16±4	···	···	···
	···	···	···	···	1994	−8	37,18±2	···	···	···
	···	···	···	···	1994	+2	63,39±3	···	···	···
	···	···	···	···	1994	+9	31,16±4	···	···	···
	···	···	···	···	1994	+18	53,36±2	···	···	···
	···	···	···	···	1994	+27	47,38±6	···	···	···
HD 75009	···	···	···	···	1994	−28	44,21±1	···	···	···
	···	···	···	···	1994	−19	22,10±2	···	···	···
	···	···	···	···	1994	−6	9±1,<6	···	···	···
	···	···	···	···	1994	+6	44,24±2	···	···	···
HD 75149	···	···	···	···	1994	−17	22,16±1	···	···	···
	···	···	···	···	1994	−9	66,30±1	···	···	···
	1971-77	+8	540,512	1,p	1994	+9	407,375±2	···	···	···
	<1971	+9	813,742	4,p	···	···	···	···	···	···
	···	···	···	···	1994	+101	<6,<6	···	···	···
HD 75241	···	···	···	···	1994	−24	190,147±1	···	···	···
	···	···	···	···	1994	−6	27,15±1	···	···	···
	···	···	···	···	1994	+7	36,22±1	···	···	···
	···	···	···	···	1994	+29	102,88±1	···	···	···
HD 75387	···	···	···	···	1994	−39	21,11±1	···	···	···
	···	···	···	···	1994	−4	12±1,<6	···	···	···
	···	···	···	···	1994	+4	68,35±1	···	···	···
HD 75759	···	···	···	···	1994	−40	13,5±1	···	···	···
	···	···	···	···	1994	−19	7±1,<6	···	···	···
	1971-77	+6	247,165	1,p	1994	+4	123,90±1	···	···	···
	···	···	···	···	1994	+12	137,115±1	···	···	···
HD 75821	···	···	···	···	1993	−98	9,6±1	1996	−99	11,6±1
	···	···	···	···	1993	−86	4,3±1	1996	−85	2±1,<1
	···	···	···	···	1993	−10	43,27±1	1996	−11	42,28±1

TABLE 3—*Continued*

Star	Obsv. Year	V_{LSR} ($km\,s^{-1}$)	$W_\lambda(D_2,D_1)$ (mÅ)	Ref.,[a] Det.	Obsv. Year	V_{LSR}[b] ($km\,s^{-1}$)	$W_\lambda(D_2,D_1)$ (mÅ)	Obsv. Year	V_{LSR}[b] ($km\,s^{-1}$)	$W_\lambda(D_2,D_1)$ (mÅ)
	···	···	···	···	1993	+1	33,15±1	1996	0	30,20±1
	1971-77	+4	232,132	1,p	···	···	···	···	···	···
	<1971	+10	240,130	4,p	1993	+10	93,51±1	1996	+9	78,43±1
	···	···	···	···	1993	+24	76,51±1	1996	+23	76,51±1
	<1971	···	<50,<50	4,p	···	···	···	···	···	···
HD 76004	···	···	···	···	1994	−17	107,49±1	···	···	···
	···	···	···	···	1994	+5	50,28±2	···	···	···
HD 76161	···	···	···	···	1993	−6	94,32±1	···	···	···
	···	···	···	···	1993	+9	395,365±1	···	···	···
	···	···	···	···	1993	+27	61,32±1	···	···	···
HD 76534	···	···	···	···	1994	−27	25,11±1	···	···	···
	···	···	···	···	1994	−16	10±2,<6	···	···	···
	···	···	···	···	1994	−5	14±2,<6	···	···	···
	···	···	···	···	1994	+8	180,170±4	···	···	···
	···	···	···	···	1994	+17	101,93±5	···	···	···
HD 76566	···	···	···	···	1994	−25	13±1,<6	···	···	···
	1971-77	−12	195,98	1,p	···	···	···	···	···	···
	···	···	···	···	1994	−9	39,11±1	···	···	···
	···	···	···	···	1994	+5	51,20±1	···	···	···
HD 78005	···	···	···	···	1994	−6	65,21±1	···	···	···
	···	···	···	···	1994	+11	75,52±1	···	···	···
	···	···	···	···	1994	+35	7±1,<6	···	···	···
HD 79275	···	···	···	···	1994	−29	18±1,<6	···	···	···
	···	···	···	···	1994	−14	129,72±1	···	···	···
	···	···	···	···	1994	−2	95,50±1	···	···	···
	···	···	···	···	1994	+102	12±1,<6	···	···	···

[a]Reference and Instrument definitions are at the end of Table 2.
[b]The velocity listed for each spectral line is the average LSR velocity for the D_1 and D_2 lines.
[c]Very uncertain due to blending.

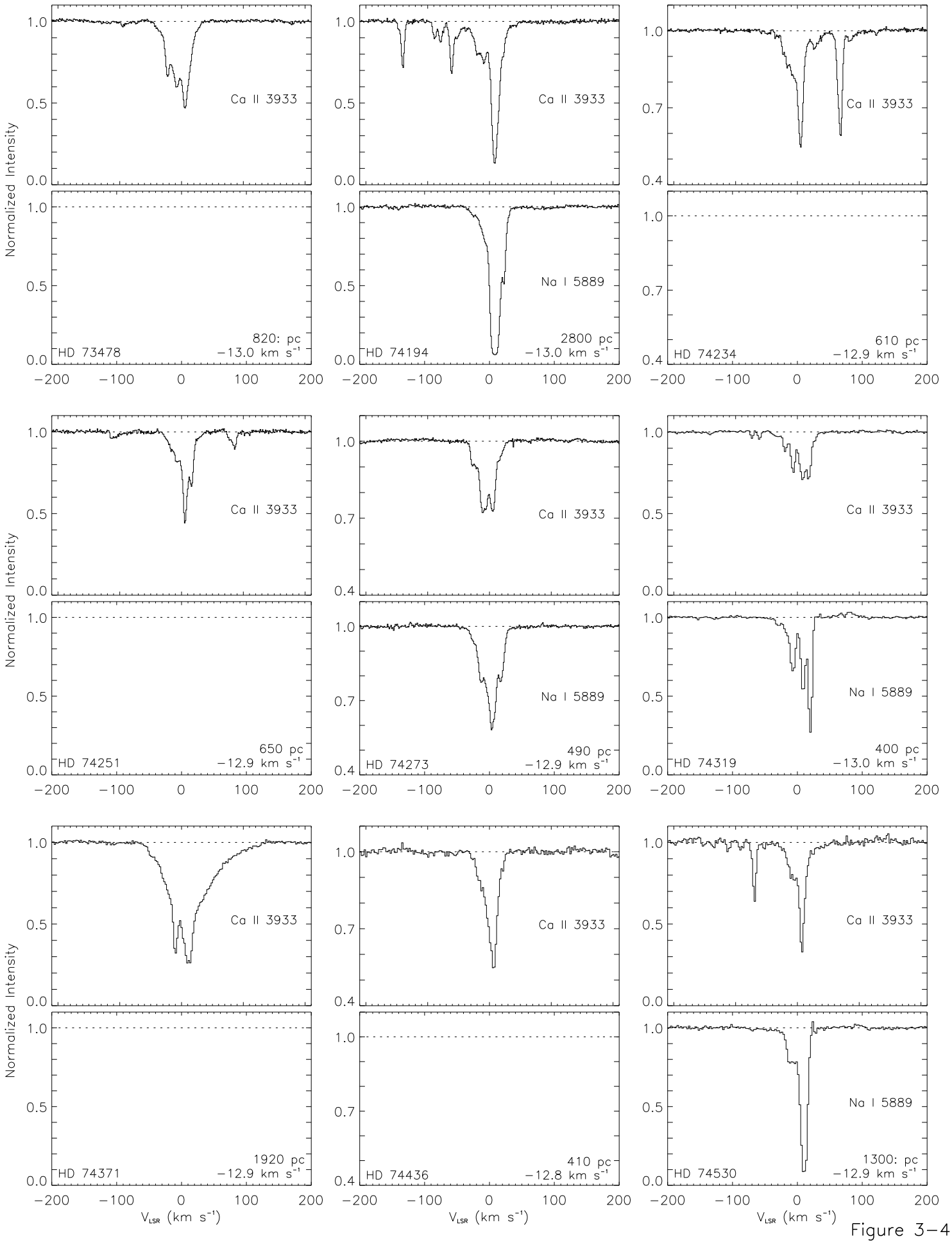
Normalized Intensity
Ca II 3933
Na I 5889
HD 73478
820: pc
−13.0 km s−1
HD 74194
2800 pc
−13.0 km s−1
HD 74234
610 pc
−12.9 km s−1
HD 74251
650 pc
−12.9 km s−1
HD 74273
490 pc
−12.9 km s−1
HD 74319
400 pc
−13.0 km s−1
HD 74371
1920 pc
−12.9 km s−1
HD 74436
410 pc
−12.8 km s−1
HD 74530
1300: pc
−12.9 km s−1
VLSR (km s−1)

Figure 3–4

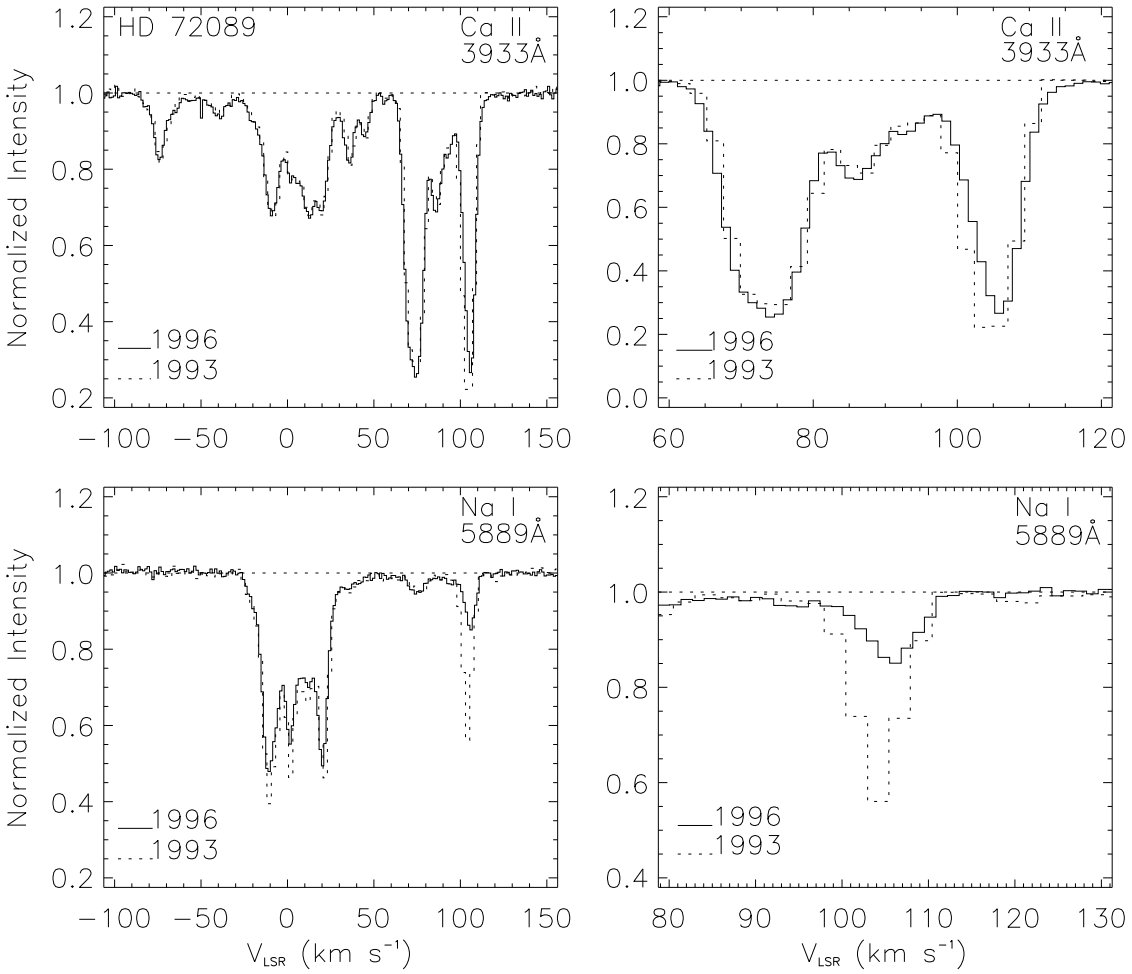
HD 72089
Ca II
3933Å
Ca II
3933Å
Na I
5889Å
Na I
5889Å
1996
1993
Normalized Intensity
V_{LSR} (km s^{-1})

Figure 4

arXiv:astro-ph/9909128v1 7 Sep 1999

TABLE 4
Absorption Lines Showing Time Variability

Star	Obsv. Year	V_{LSR} ($km\,s^{-1}$)	N(Ca II) ($10^{11}\,cm^{-2}$)	W_λ(K) (mÅ)	V_{LSR} ($km\,s^{-1}$)	N(Na I) ($10^{11}\,cm^{-2}$)	$W_\lambda(D_2)$ (mÅ)	$W_\lambda(D_1)$ (mÅ)	ΔV_{LSR} [a] ($km\,s^{-1}$)
HD 72089	1993	+105	10±.1	90±1	+104	2.9±.1	56±2	30±2	−13.4
	1996	+106	8.6±.1	75±1	+106	1.2±.1	23±1	9±1	
HD 72127A	1994	−28	8.2±.1	71±1	···	···	···	···	−13.4
	1996	−28	10±.1	92±1	···	···	···	···	
	1994	−21	11±.1	97±1	···	···	···	···	
	1996	−21	13±.1	126±1	···	···	···	···	
	1994	−10	8.7±.1	76±1	···	···	···	···	
	1996	−10	7.8±.1	68±1	···	···	···	···	
HD 72997	1991	+189	2.4±.1	21±1	+189	0.77±.1	15±1	8±1	−13.3
	1993	+190	2.6±.1	23±1	+190	0.83±.1	16±1	<6	
	1996	+191	2.1±.1	19±1	+191	0.77±.1	15±1	7±1	
HD 73658	1993	−33	5.1±.1	41±1	···	···	···	···	−13.1
	1996	−32	0.4±.2	4±2	···	···	···	···	
	1993	−15	22±.1	144±1	···	···	···	···	
	1996	−15	14±.1	91±1	···	···	···	···	
HD 74455	1994	−173	5.1±.1	32±1	···	···	···	···	−12.9
	1996	−173	3.1±.1	23±1	···	···	···	···	
HD 75309	1993	−118	1.4±.1	12±1	···	···	···	···	−12.8
	1996	−120	1.8±.1	16±1	···	···	···	···	
	1993	+81	0.4±.2	4±2	···	···	···	···	
	1996	+81	<0.1	<3	···	···	···	···	
	1993	+89	0.7±.2	7±2	···	···	···	···	
	1996	+89	<0.1	<3	···	···	···	···	
HD 75821	1993	−98	2.4±.1	21±1	−98	0.5±.1	9±1	6±1	−12.7
	1996	−99	3.0±.1	26±1	−99	0.6±.1	11±1	6±1	
	1993	−85	7.6±.1	66±1	−86	0.3±.1	4±1	3±1	
	1996	−85	6.1±.1	53±1	−85	0.1±.1	2±1	<1	

[a]LSR-to-heliocentric velocity conversion factor where $V_{LSR} = V_{helio} + \Delta V_{LSR}$.

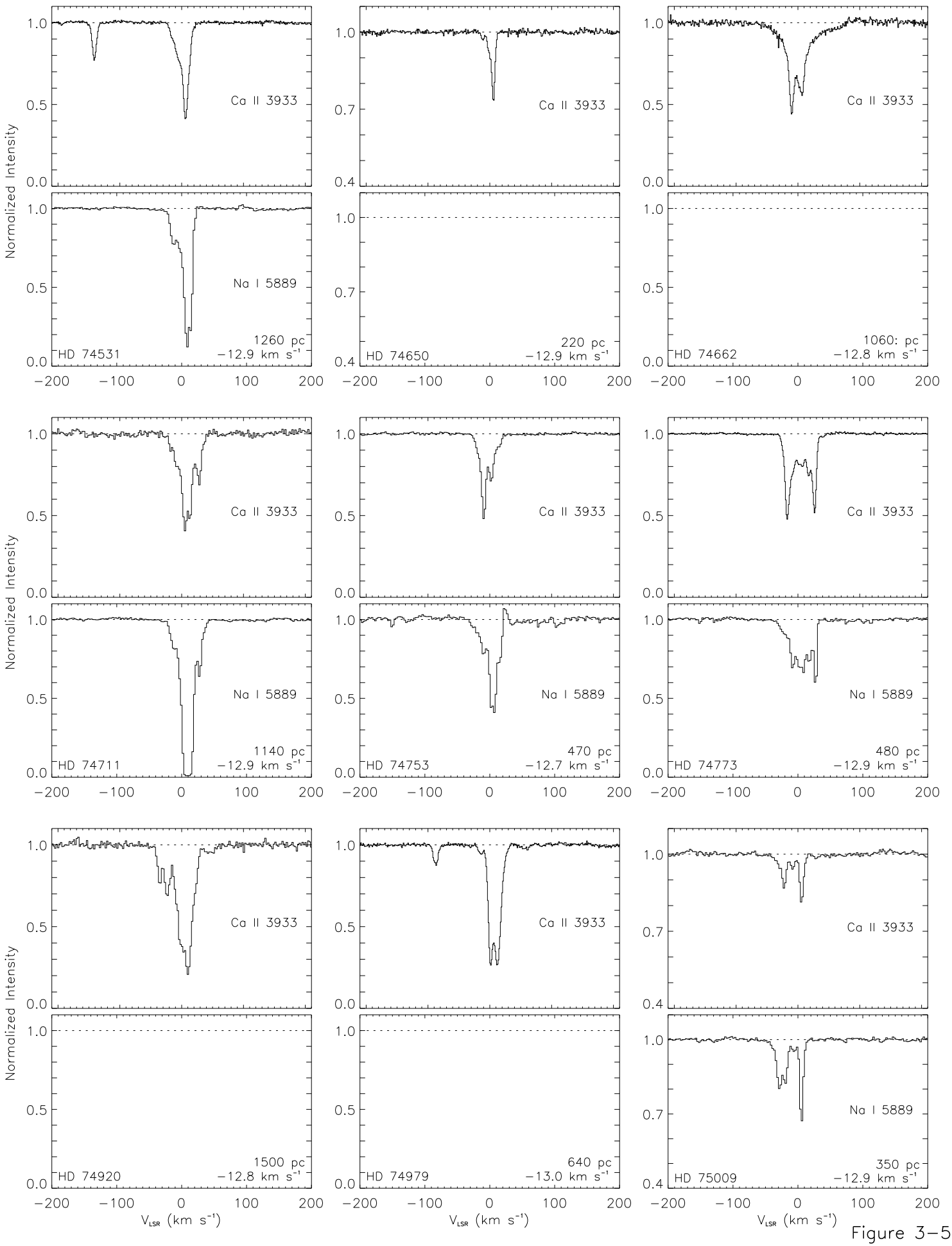
Normalized Intensity
Ca II 3933
Na I 5889
HD 74531
1260 pc
−12.9 km s−1
HD 74650
220 pc
−12.9 km s−1
HD 74662
1060: pc
−12.8 km s−1
HD 74711
1140 pc
−12.9 km s−1
HD 74753
470 pc
−12.7 km s−1
HD 74773
480 pc
−12.9 km s−1
HD 74920
1500 pc
−12.8 km s−1
HD 74979
640 pc
−13.0 km s−1
HD 75009
350 pc
−12.9 km s−1
VLSR (km s−1)

Figure 3–5

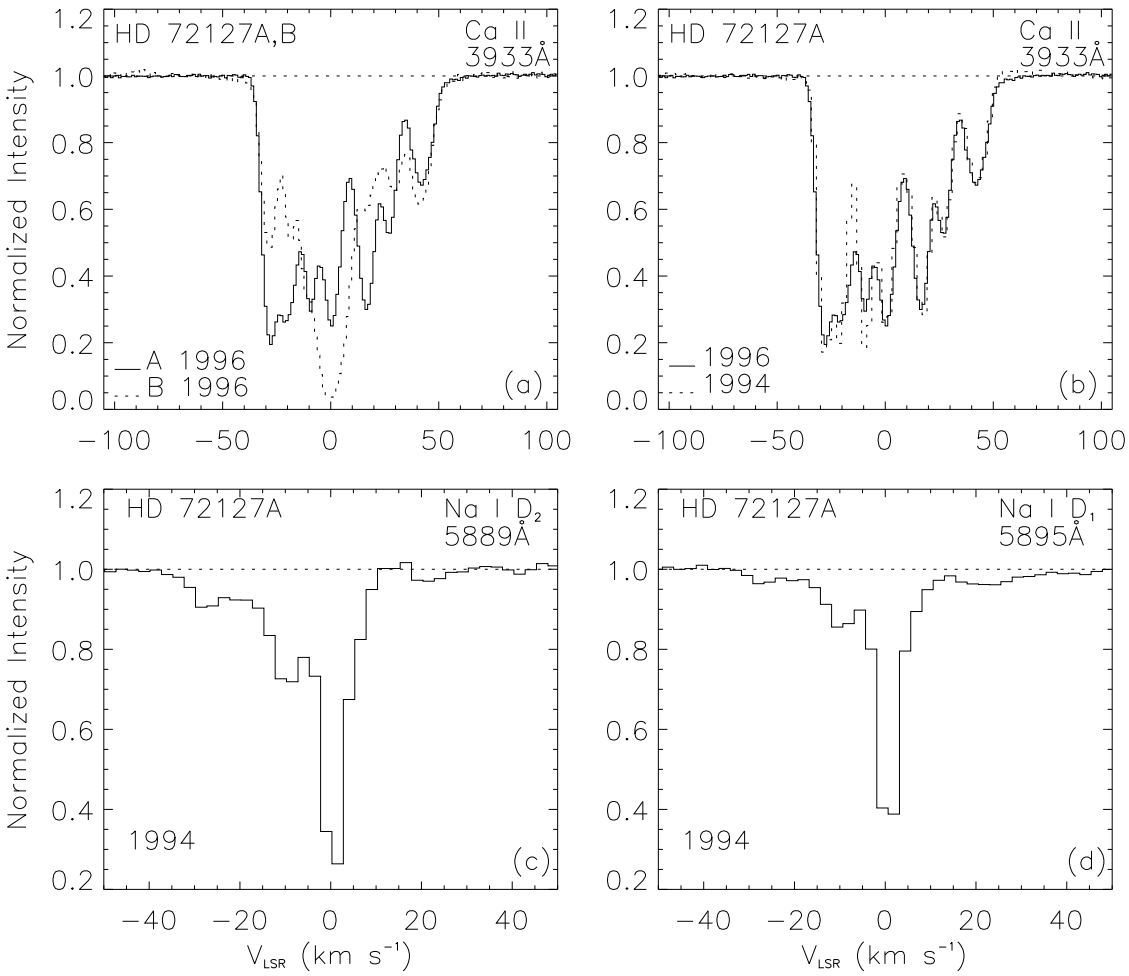
HD 72127A,B
Ca II
3933Å
A 1996
B 1996
(a)
HD 72127A
Ca II
3933Å
1996
1994
(b)
HD 72127A
Na I D2
5889Å
1994
(c)
HD 72127A
Na I D1
5895Å
1994
(d)
Normalized Intensity
VLSR (km s−1)

Figure 5

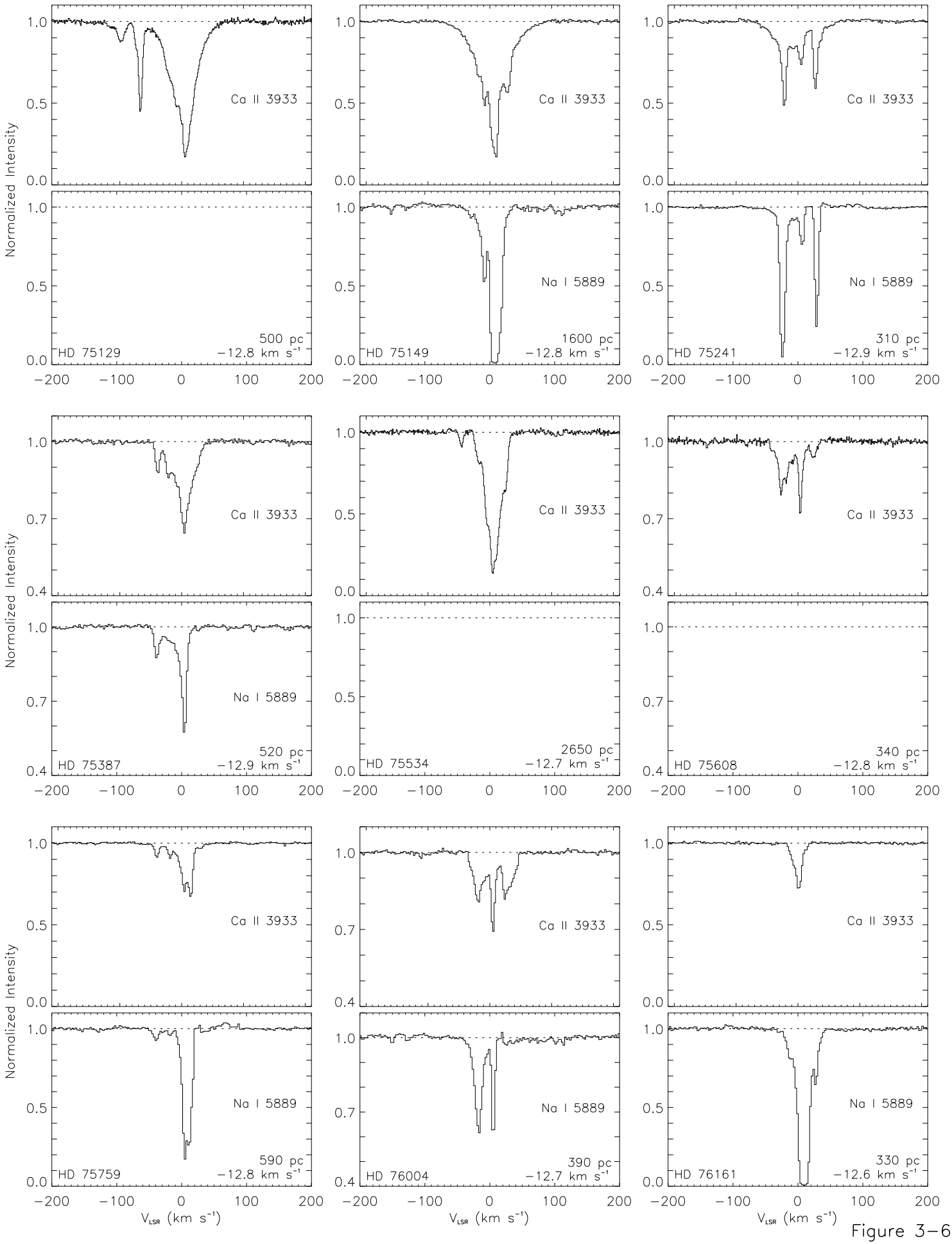
Normalized Intensity
Ca II 3933
Na I 5889
HD 75129
500 pc
−12.8 km s−1
HD 75149
1600 pc
−12.8 km s−1
HD 75241
310 pc
−12.9 km s−1
HD 75387
520 pc
−12.9 km s−1
HD 75534
2650 pc
−12.7 km s−1
HD 75608
340 pc
−12.8 km s−1
HD 75759
590 pc
−12.8 km s−1
HD 76004
390 pc
−12.7 km s−1
HD 76161
330 pc
−12.6 km s−1
VLSR (km s−1)

Figure 3–6

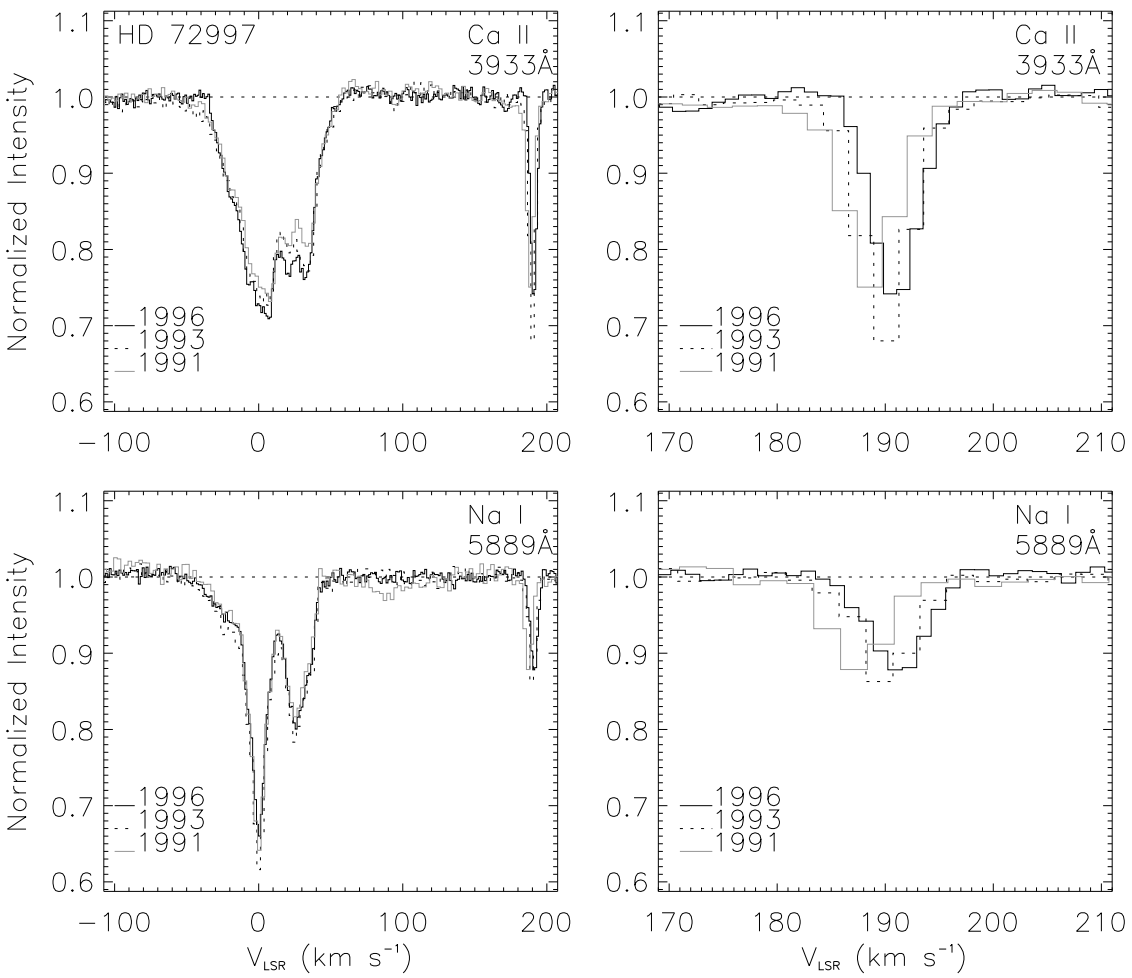
HD 72997
Ca II
3933Å
Ca II
3933Å
Na I
5889Å
Na I
5889Å
1996
1993
1991
Normalized Intensity
V_{LSR} (km s^{-1})

Figure 6

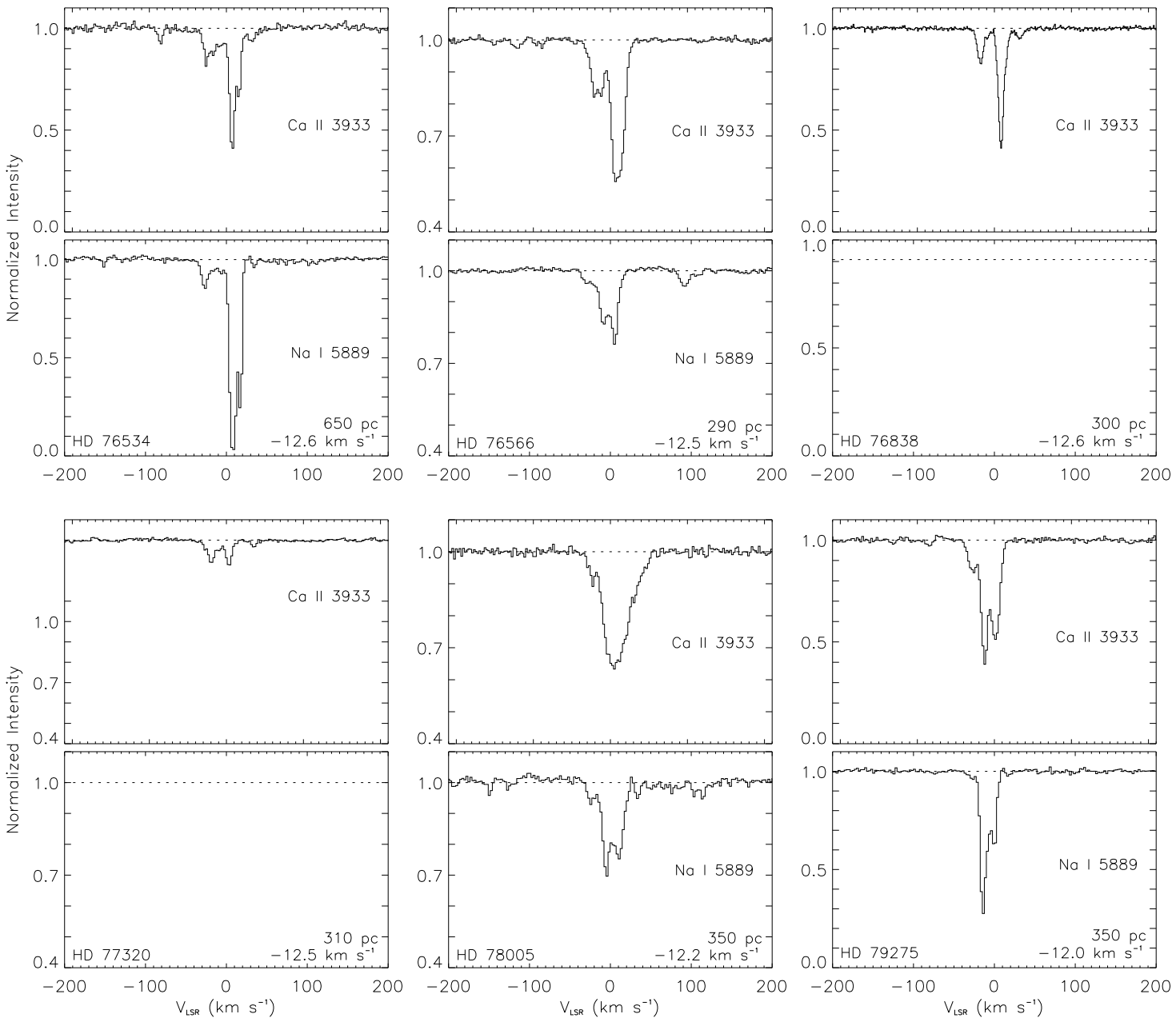
Normalized Intensity
Ca II 3933
Na I 5889
HD 76534
650 pc
−12.6 km s⁻¹
HD 76566
290 pc
−12.5 km s⁻¹
HD 76838
300 pc
−12.6 km s⁻¹
HD 77320
310 pc
−12.5 km s⁻¹
HD 78005
350 pc
−12.2 km s⁻¹
HD 79275
350 pc
−12.0 km s⁻¹
V_LSR (km s⁻¹)

Figure 3–7

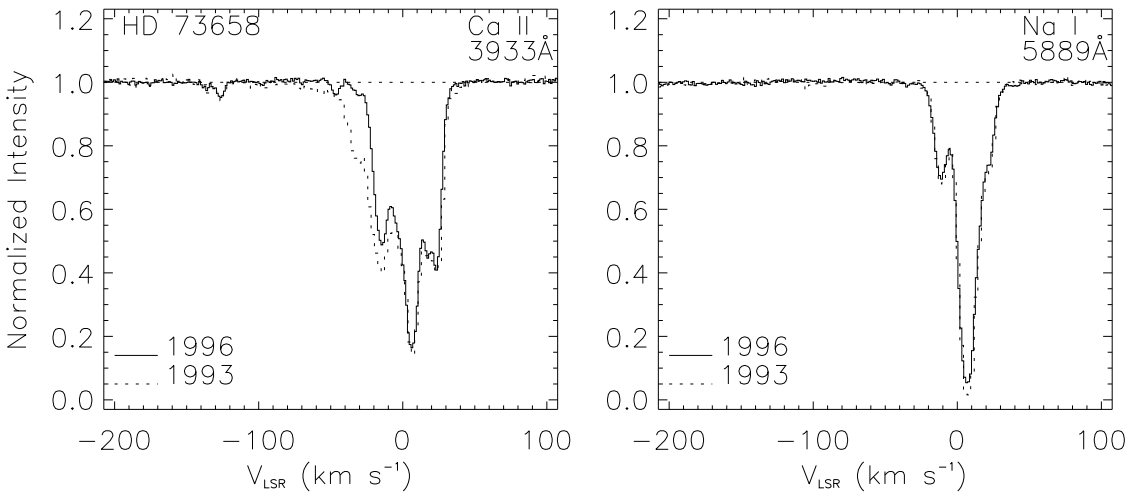
HD 73658
Ca II
3933Å
Na I
5889Å
1996
1993
Normalized Intensity
V_{LSR} (km s^{-1})
1.2
1.0
0.8
0.6
0.4
0.2
0.0
−200
−100
0
100

Figure 7

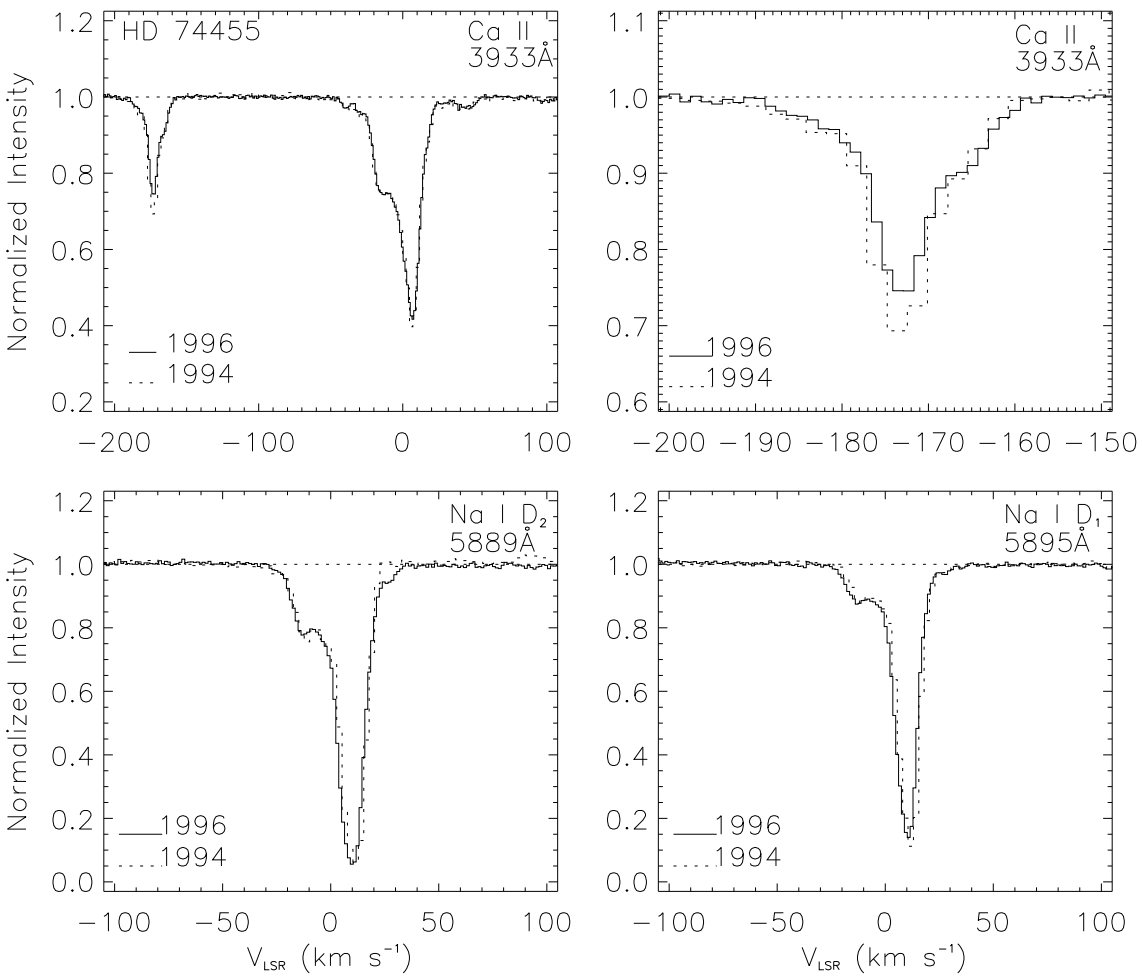
HD 74455
Ca II
3933Å
Ca II
3933Å
Na I D2
5889Å
Na I D1
5895Å
1996
1994
Normalized Intensity
VLSR (km s−1)

Figure 8

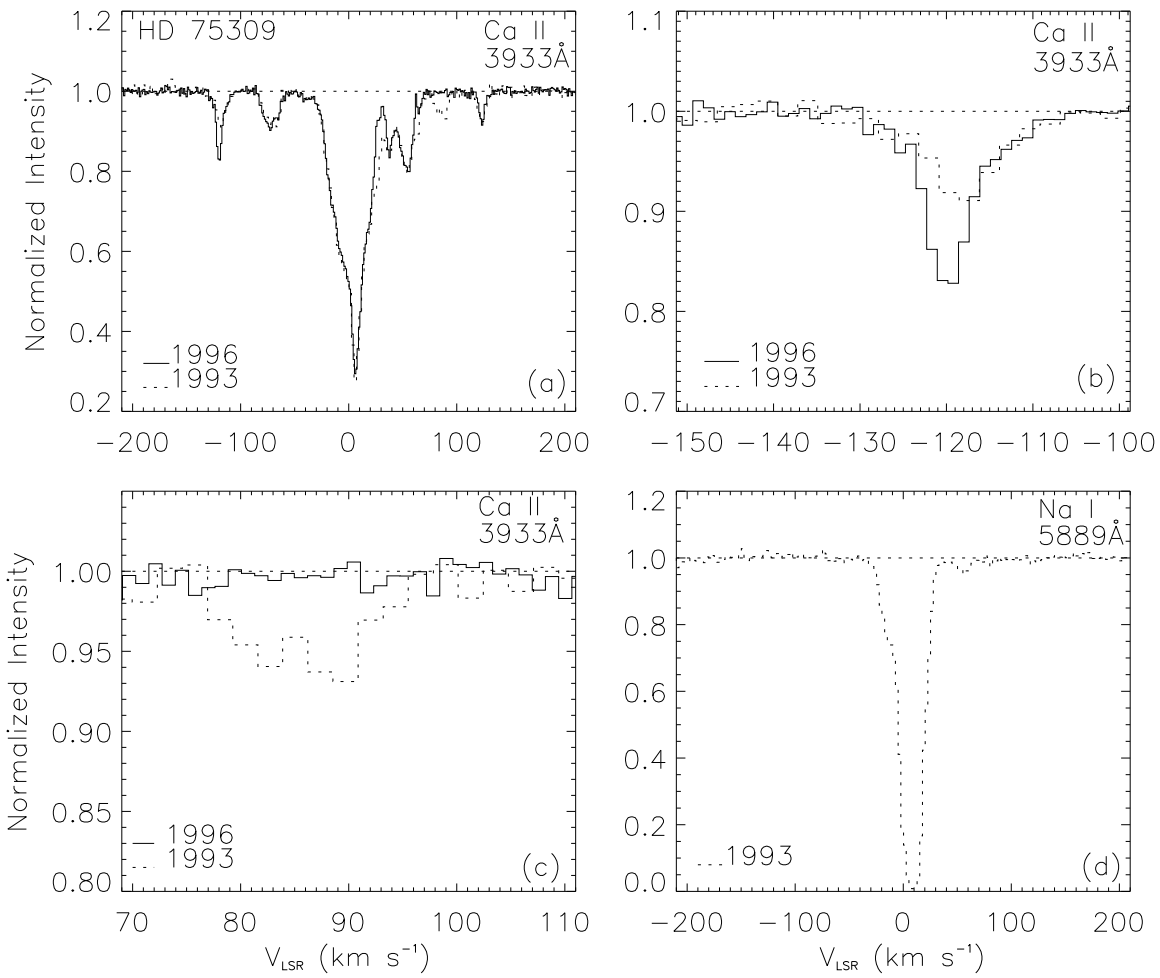
HD 75309
Ca II
3933Å
Normalized Intensity
1996
1993
(a)
Ca II
3933Å
1996
1993
(b)
Ca II
3933Å
1996
1993
(c)
Na I
5889Å
1993
(d)
V_LSR (km s^-1)
V_LSR (km s^-1)

Figure 9

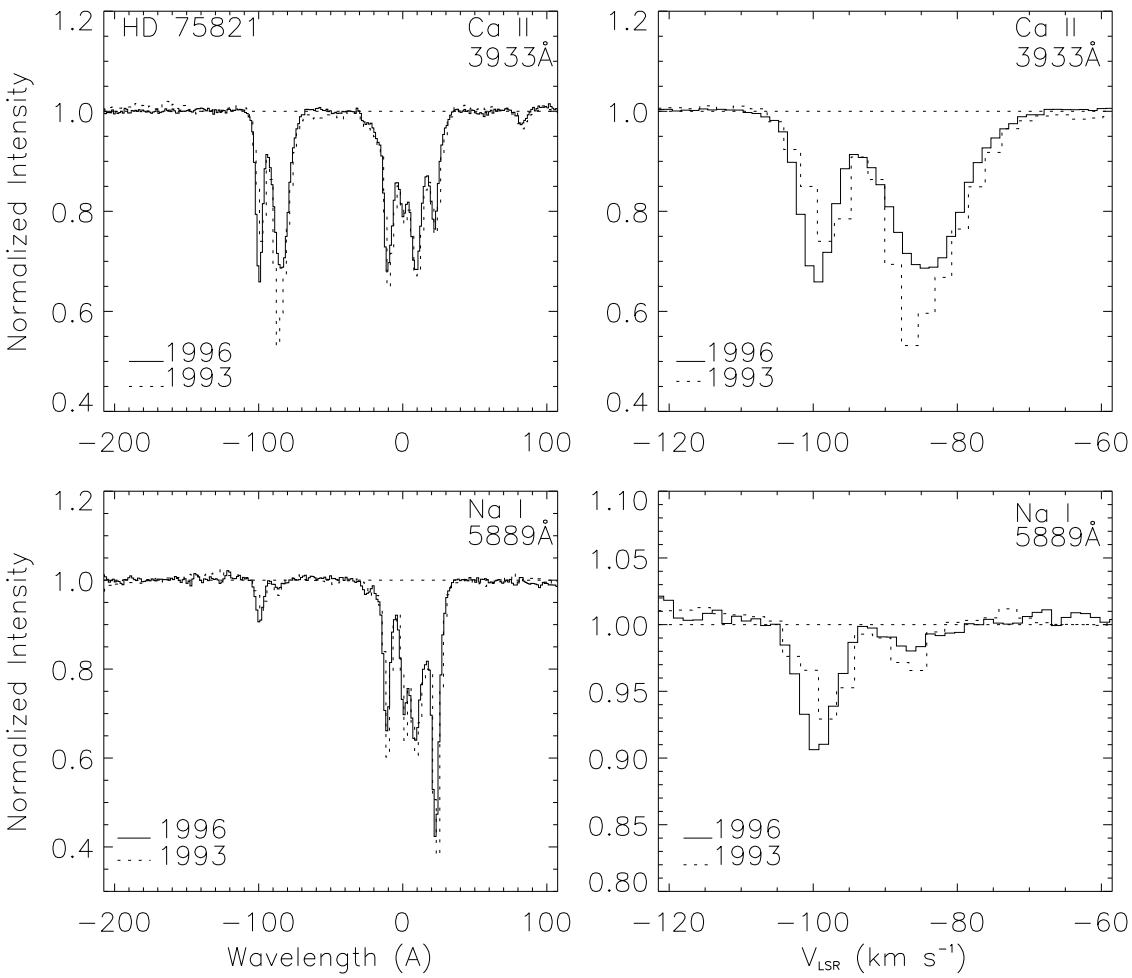
HD 75821
Ca II
3933Å
Ca II
3933Å
Na I
5889Å
Na I
5889Å
1996
1993
Normalized Intensity
Wavelength (A)
V_{LSR} (km s^{-1})

Figure 10